

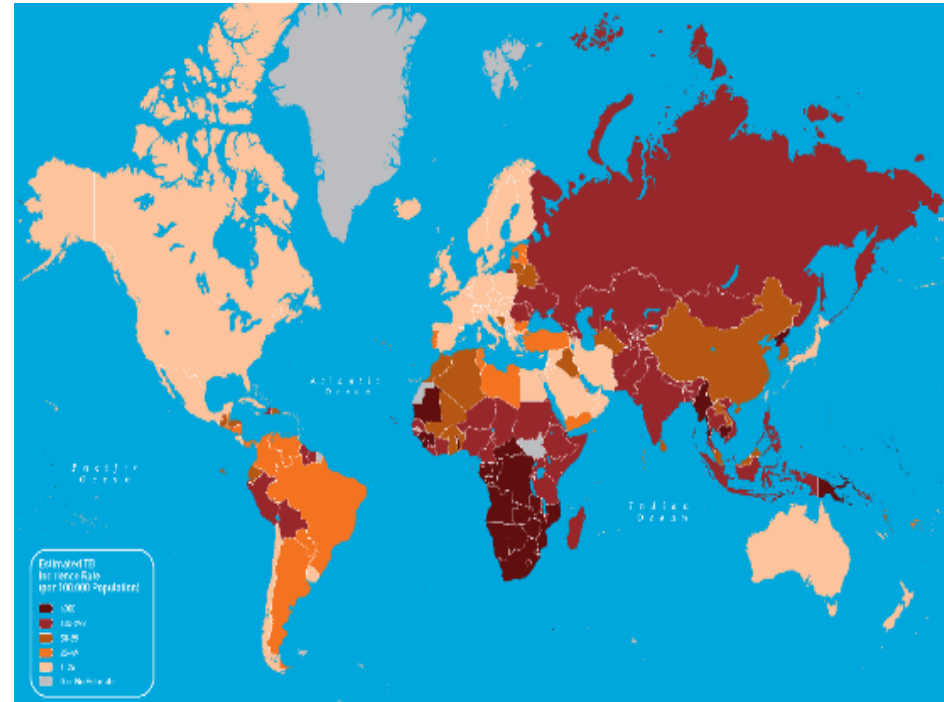
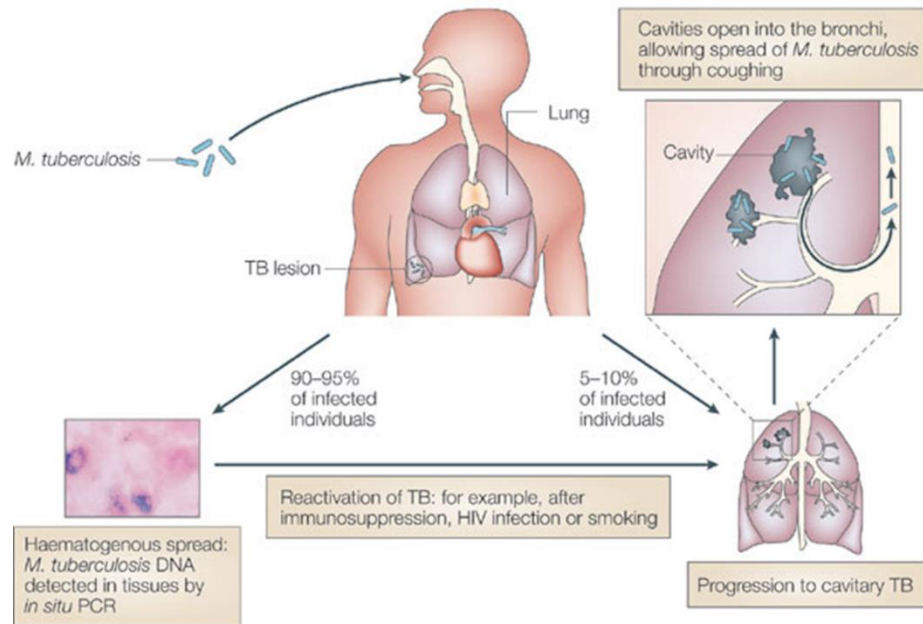
# Paper-based analytical devices and systems

## 紙張基材分析元件與系統

December 9<sup>th</sup>, 2020

# The Urgency of Tuberculosis Diagnosis and Treatment

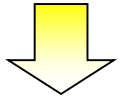
- According to the World Health Organization (WHO) Global Tuberculosis Report 2019, there were an estimated **1.3 million people died from TB in 2017 (1 million from HIV)**.
- **TB can be cured. However, HIV can't. So, how could this happen?**



Copyright © 2005 Nature Publishing Group  
Nature Reviews | Immunology

# Healthcare System

**Accurate diagnosis**  
Analytical equipment or  
symptom observed by MD



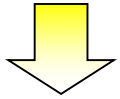
**Treatment**



[weillcornell.org](http://weillcornell.org)



[pharmacyinfo.xyz](http://pharmacyinfo.xyz)



**Prognosis**



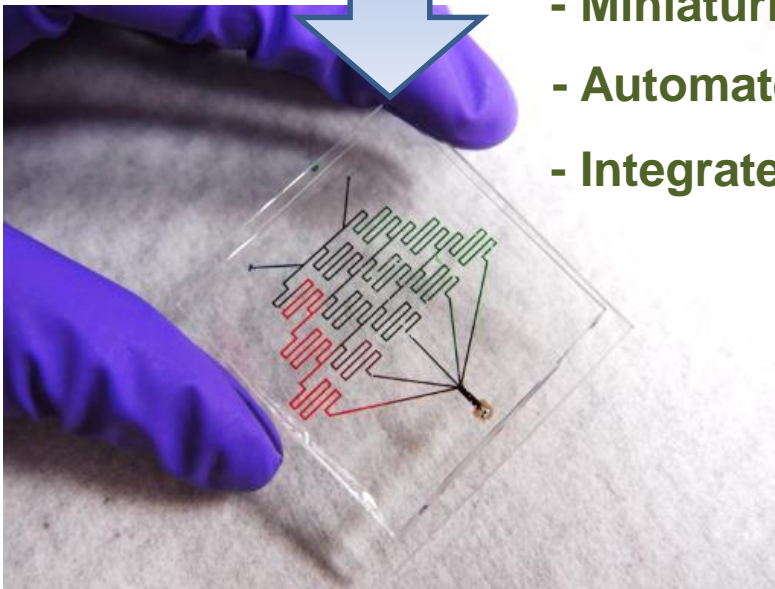
[www.mesoAdvice.org](http://www.mesoAdvice.org)

# Lab-on-a-Chip System

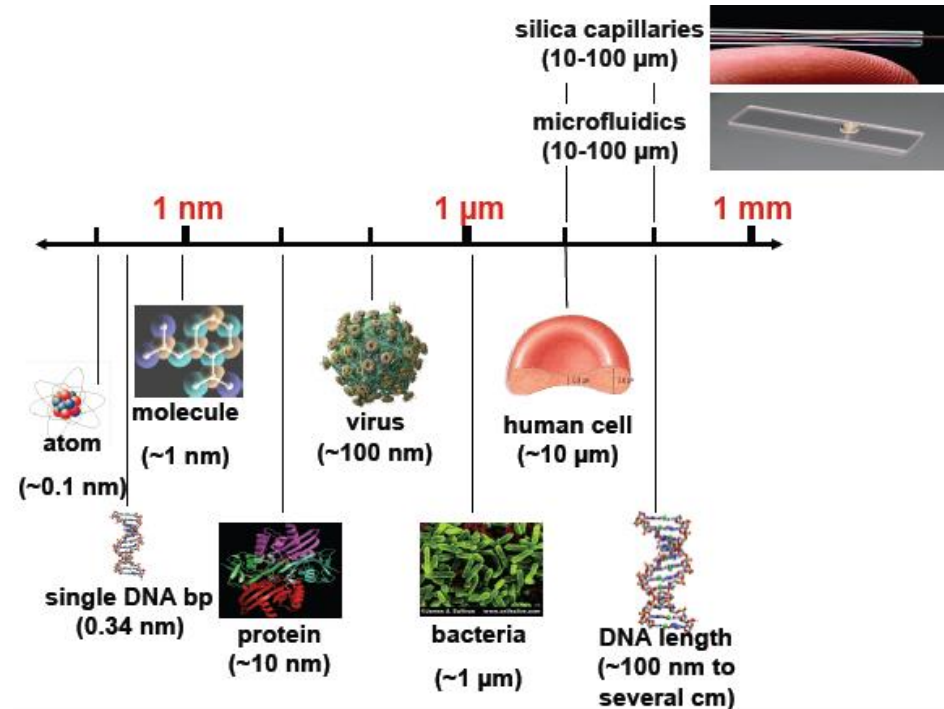


- Low fluid volumes consumption
- Faster analysis and response times
- Better process control
- Compactness of the systems
- Lower fabrication costs
- Safer platform

## Microfluidics

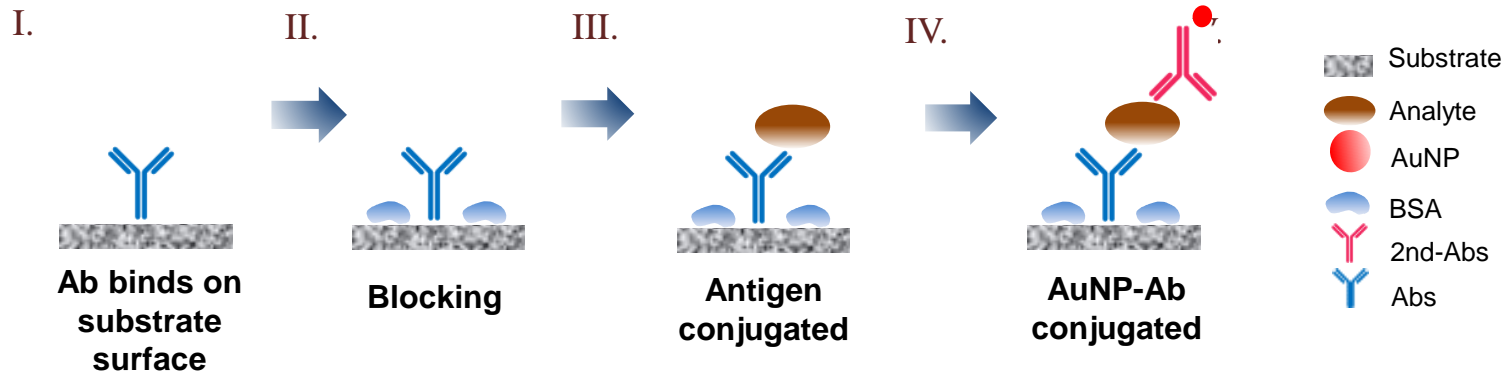


- Miniaturize
- Automate
- Integrate

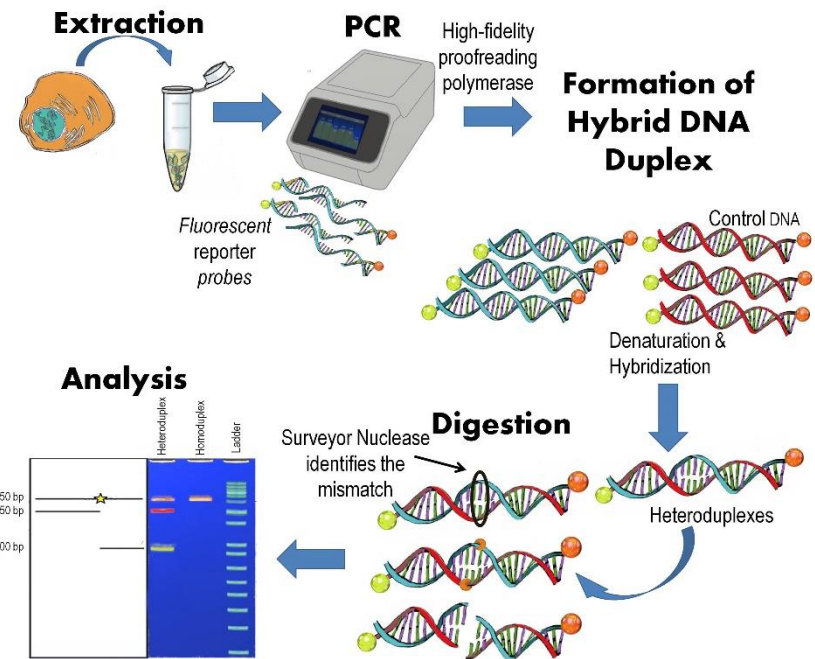
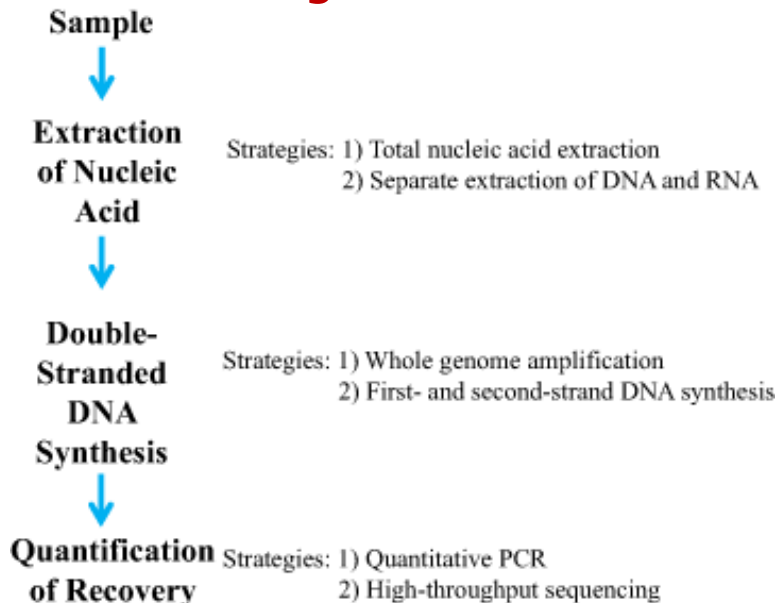


# Chemosensor & Biosensor

## Immunoassay (Protein based detection)



## Molecular Diagnosis





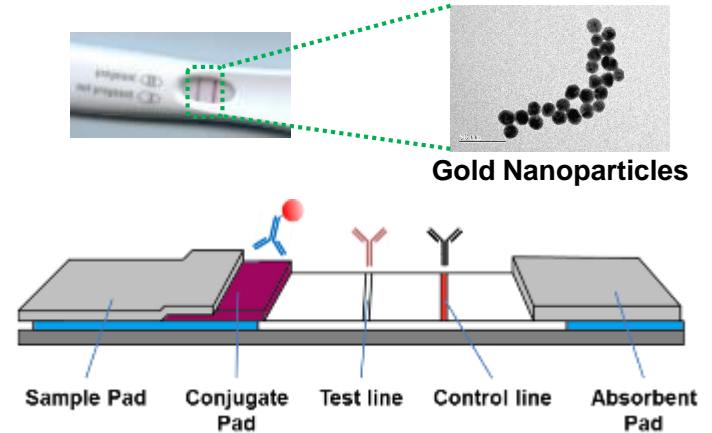
# Paper Devices

- ❖ The wettability
- ❖ White
- ❖ Simple fabrication
- ❖ Cost effective
- ❖ Portable
- ❖ Disposable
- ❖ Flexible
- ❖ Easy to store and delivery
- ❖ Scalable

## □ Dipstick



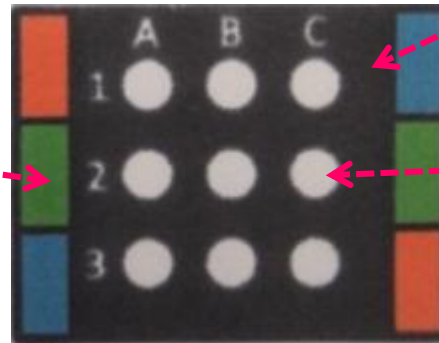
## □ Lateral Flow Immunoassay (LFA)



## □ Microfluidic Paper-Based Analytical Devices ( $\mu$ PADs)



Color bar for light condition adjustment



Hydrophobic wax for detection area definition



Hydrophilic area for colorimetric detection

# Fluid Transport in Paper

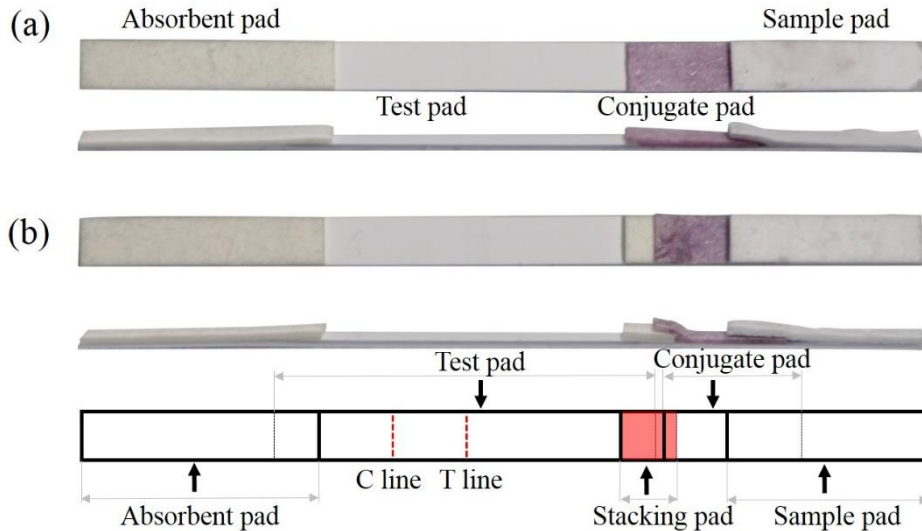
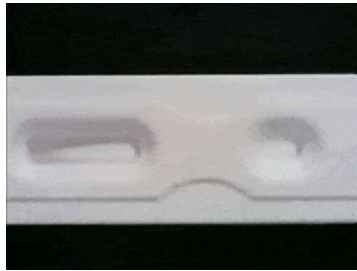
## Lucas-Washburn equation

$$\frac{dl}{dt} = \frac{\Sigma P}{8\eta l} (r^2 + 4\epsilon r) \quad P_c = \frac{2\gamma \cos\theta}{r}$$

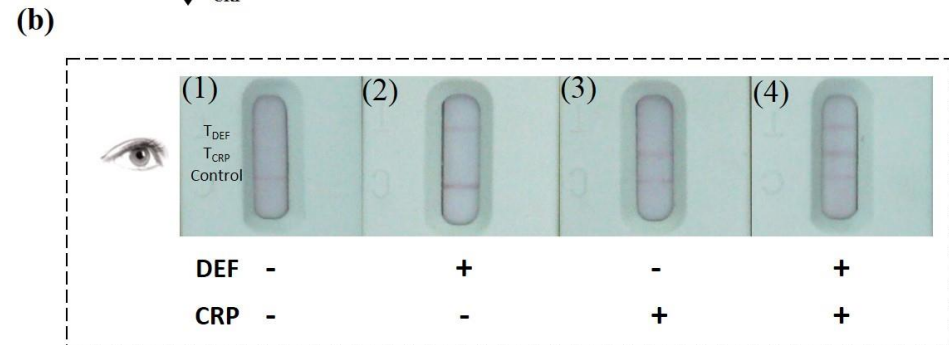
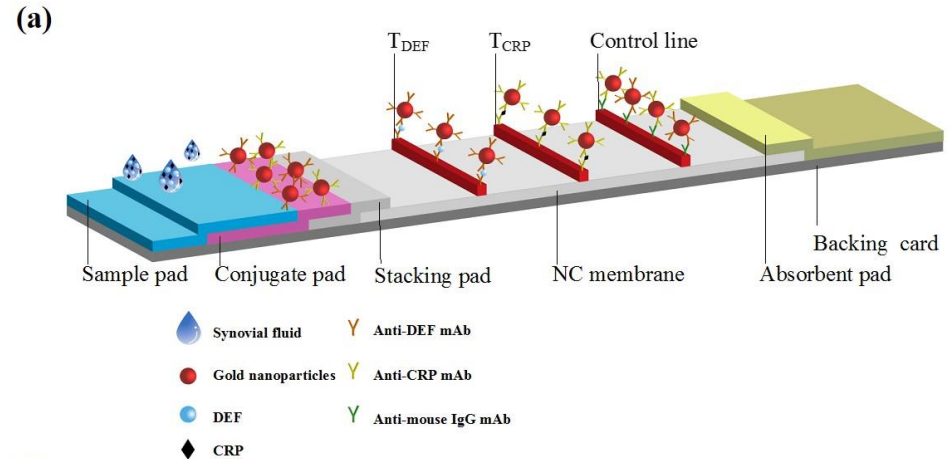
Where  $\eta$  is viscosity and  $\Sigma P$  is the sum of atmospheric pressure, hydrostatic pressure, and capillary pressure.  $\epsilon$  is the coefficient of slip,  $\gamma$  is surface tension,  $\theta$  is the solid-liquid contact angle,  $Q$  is the volumetric flow rate,  $\kappa$  is the permeability of the paper, and  $WH$  is the cross-sectional area perpendicular to the flow.

## Darcy's law

$$Q = \frac{\kappa WH}{\eta L} \Delta P$$



Scientific Reports, 2018, 17319



Scientific Reports, 2019, 15679

# Diagnosics for the Developing World: Microfluidic Paper-Based Analytical Devices

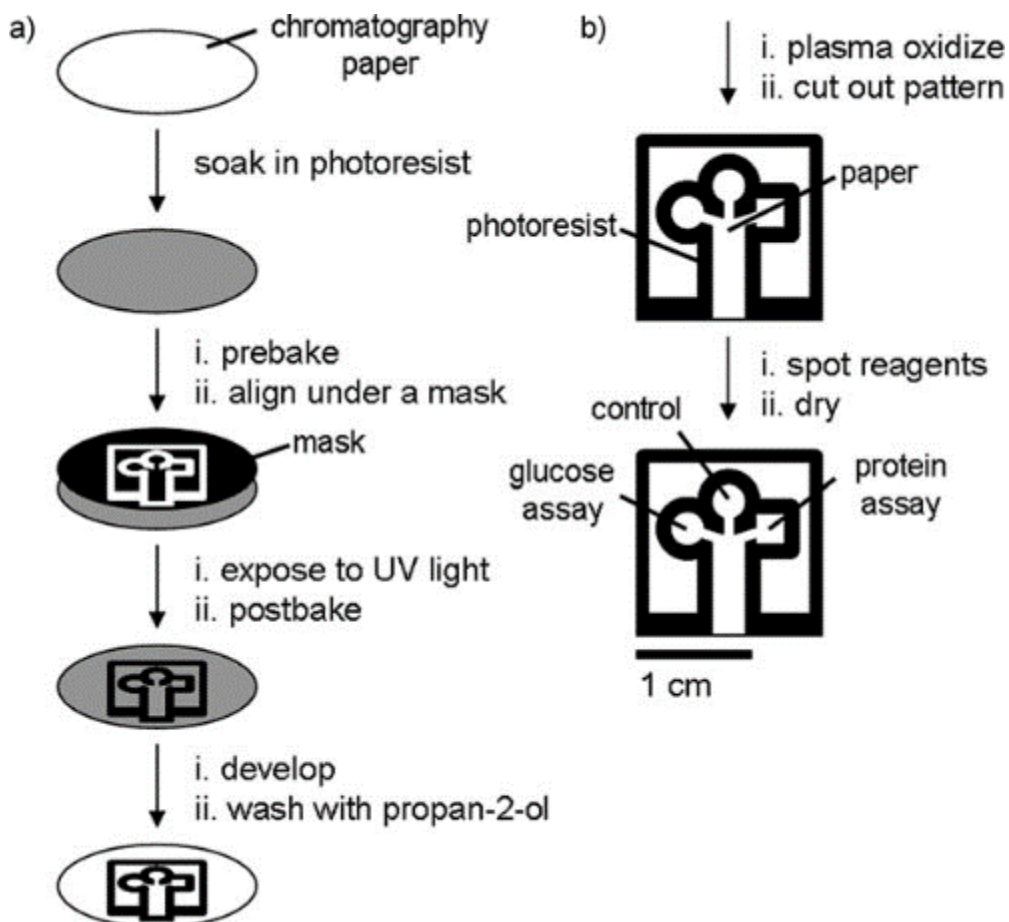
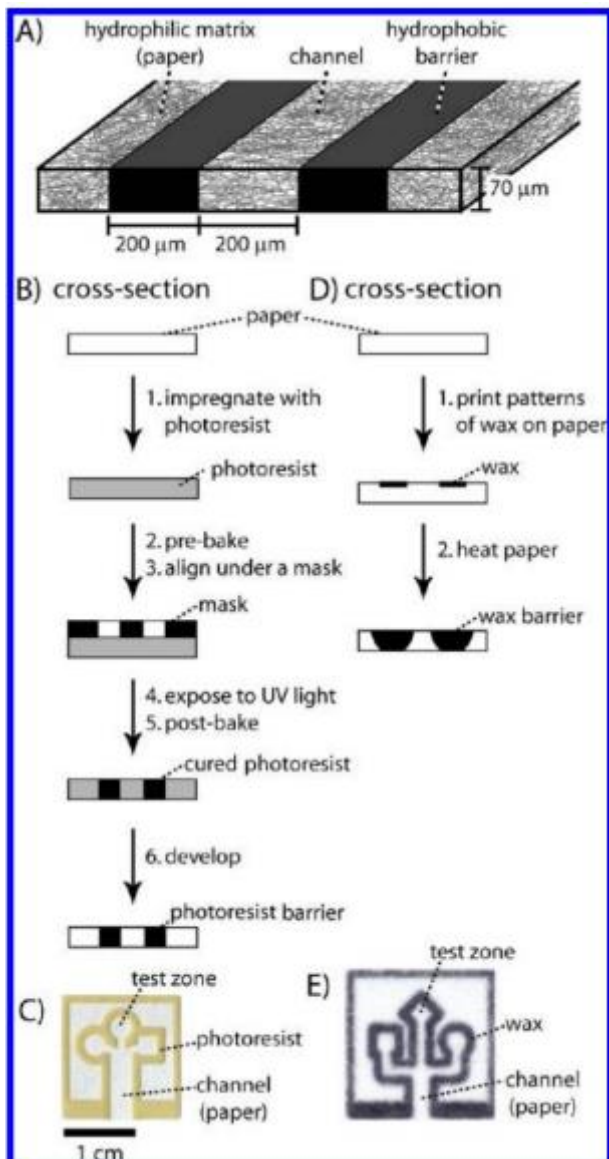


Diagram depicting the method for patterning paper into millimeter-sized channels



# Patterned Paper as a Platform for Inexpensive, Low-Volume, Portable Bioassays

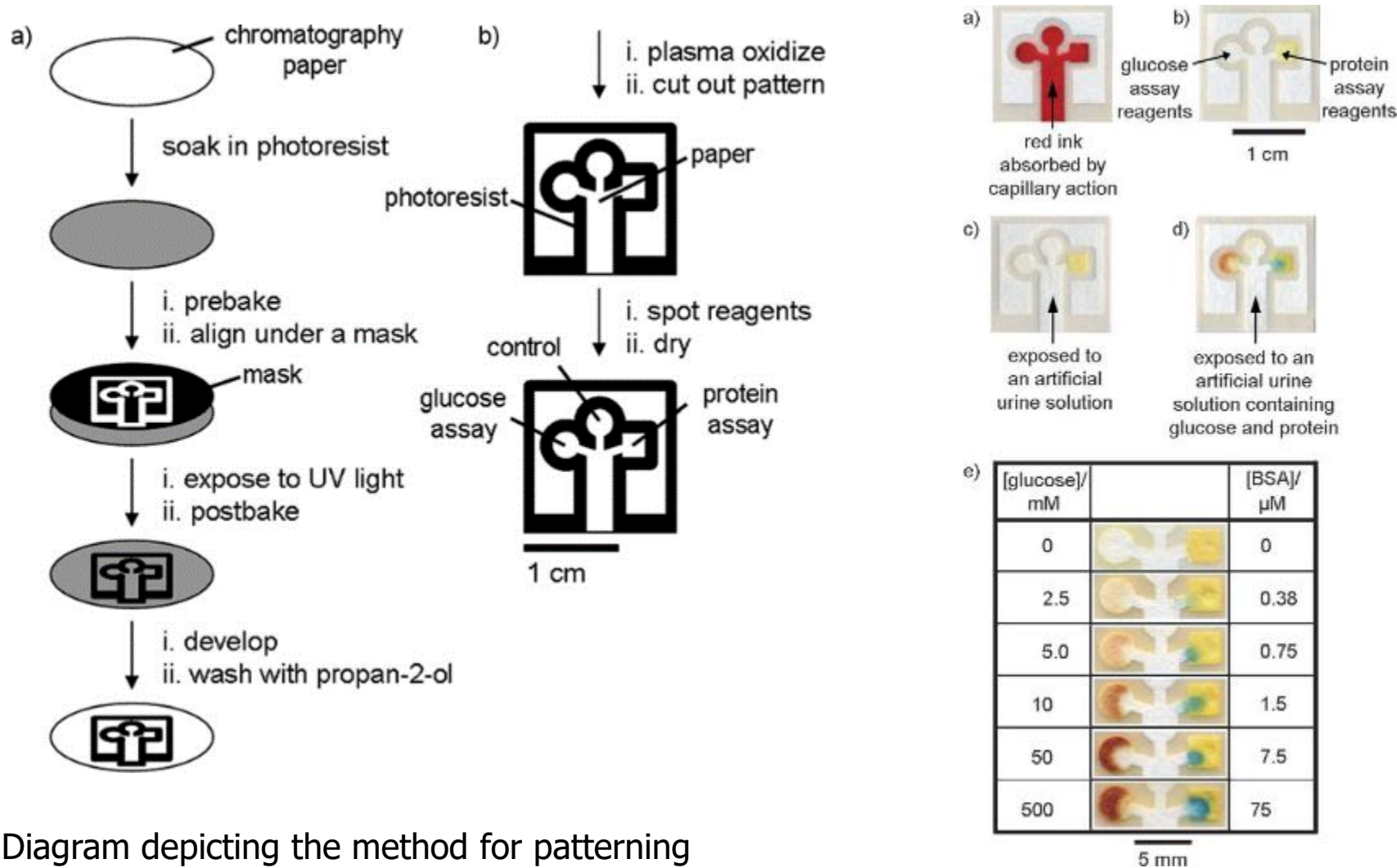
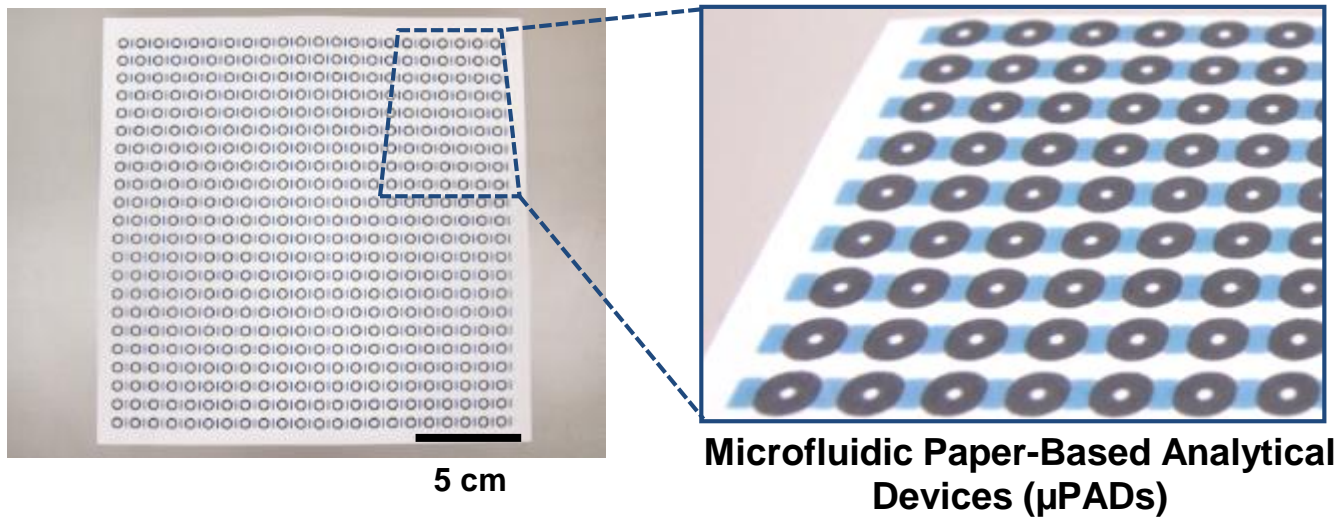


Diagram depicting the method for patterning paper into millimeter-sized channels

Chromatography paper patterned with photoresist. The darker lines are cured photoresist, whereas the lighter areas are unexposed paper.

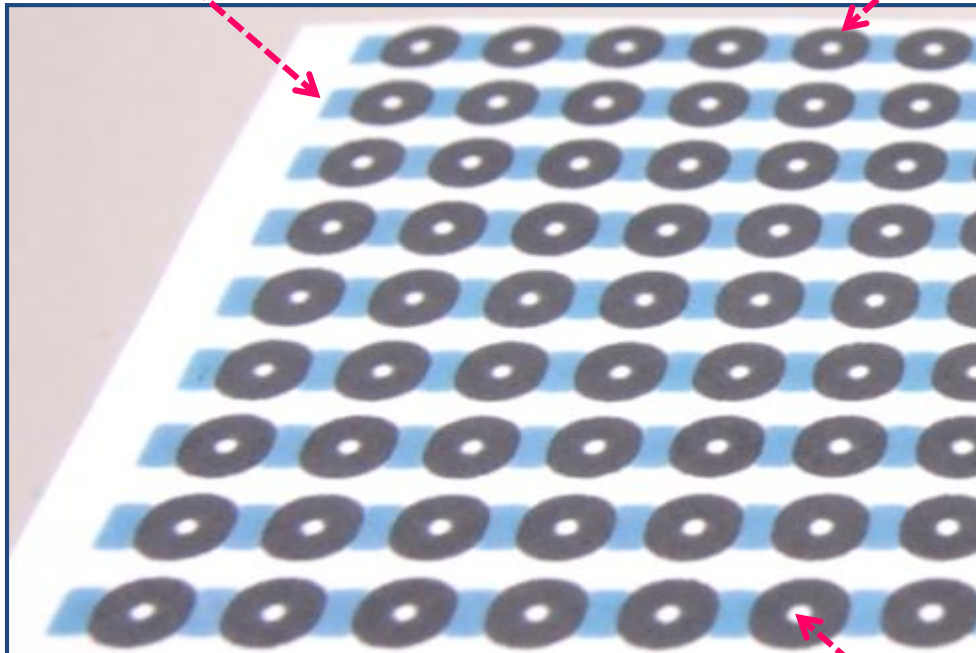
# Paper-Based Devices Fabrication



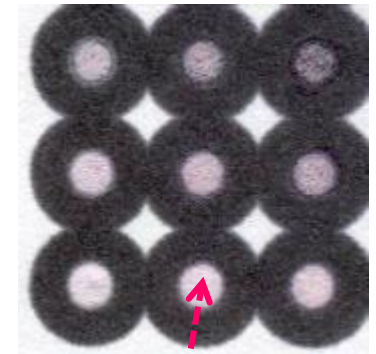
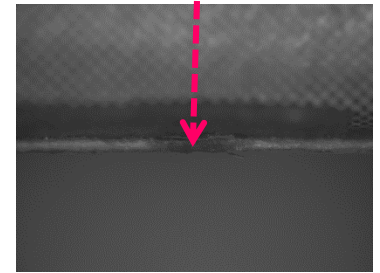
Method (References)	Channel ( $\mu\text{m}$ )	Barrier ( $\mu\text{m}$ )	Advantages	Disadvantages
Photolithography (10)	$186 \pm 13$	$248 \pm 13$	Can pattern a wide variety of papers up to $360 \mu\text{m}$ in width.	Hydrophilic areas exposed to polymers and solvents.
Plotting (30)	$\sim 1000^a$	$\sim 1000^a$	Hydrophilic channels not exposed to polymers or solvents; hydrophobic barriers are flexible.	Requires a customized plotter.
Inkjet etching (31)	$420 \pm 50$	— <sup>a</sup>	Reagents can be inkjet printed into the test zones using the printer.	Requires a customized inkjet printer; hydrophilic areas exposed to polymers and solvents.
Plasma etching (32)	$\sim 1500^a$	— <sup>a</sup>	Useful for laboratories equipped with a plasma cleaner that wish to make many replicates of a few simple patterns.	Hydrophilic areas exposed to polymers and solvents; metal masks must be made for each pattern; cannot produce arrays of free-standing hydrophobic patterns.
Cutting (29)	$1000^b$	$700^b$	Hydrophilic channels not exposed to polymers or solvents.	Devices must be encased in tape; cannot produce arrays of free-standing hydrophilic patterns.
Wax printing (33,34)	$561 \pm 45$	$850 \pm 50$	Rapid ( $\sim 5$ minutes); requires only a commercially available printer and hot plate; hydrophilic channels not exposed to polymers or solvents.	The design of the patterns must account for the spreading of the wax in the paper.

# Introduction to Microfluidic Paper-Based Analytical Devices ( $\mu$ PADs)

**Color bar for light condition**

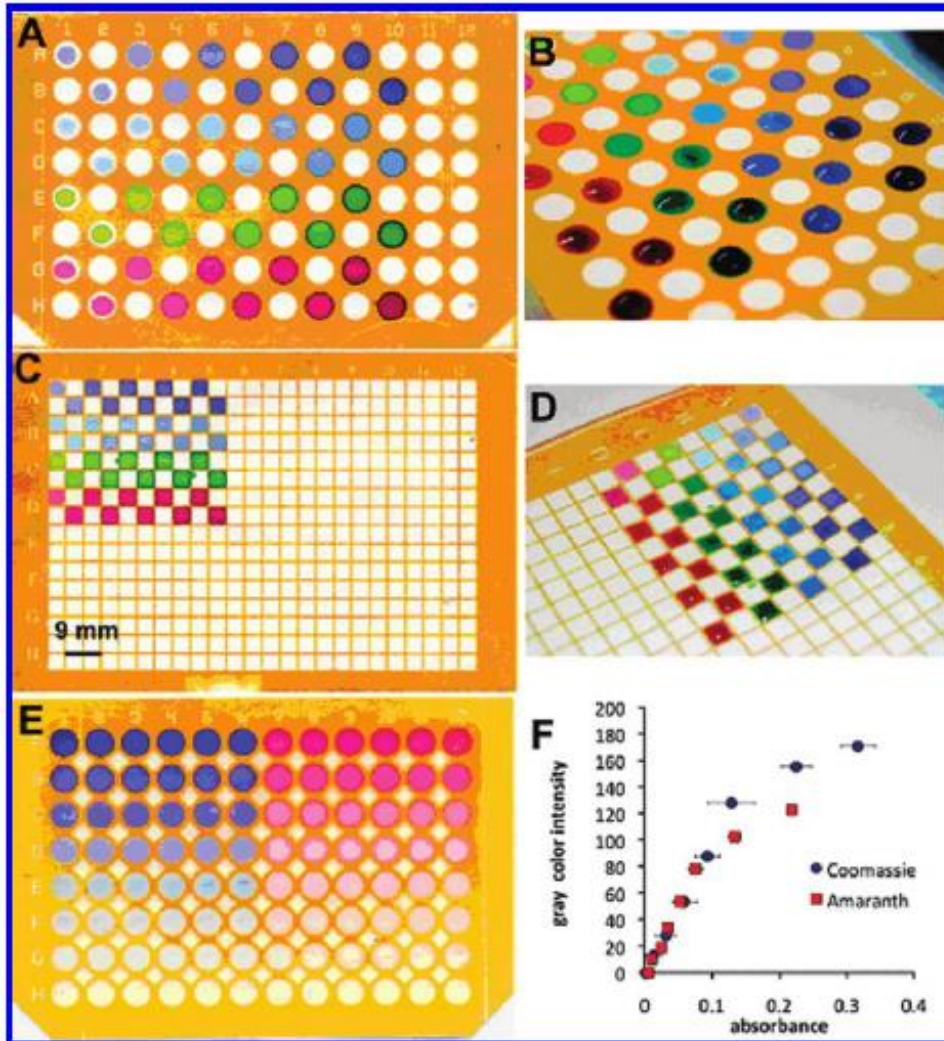


**Hydrophobic wax for detection area definition**

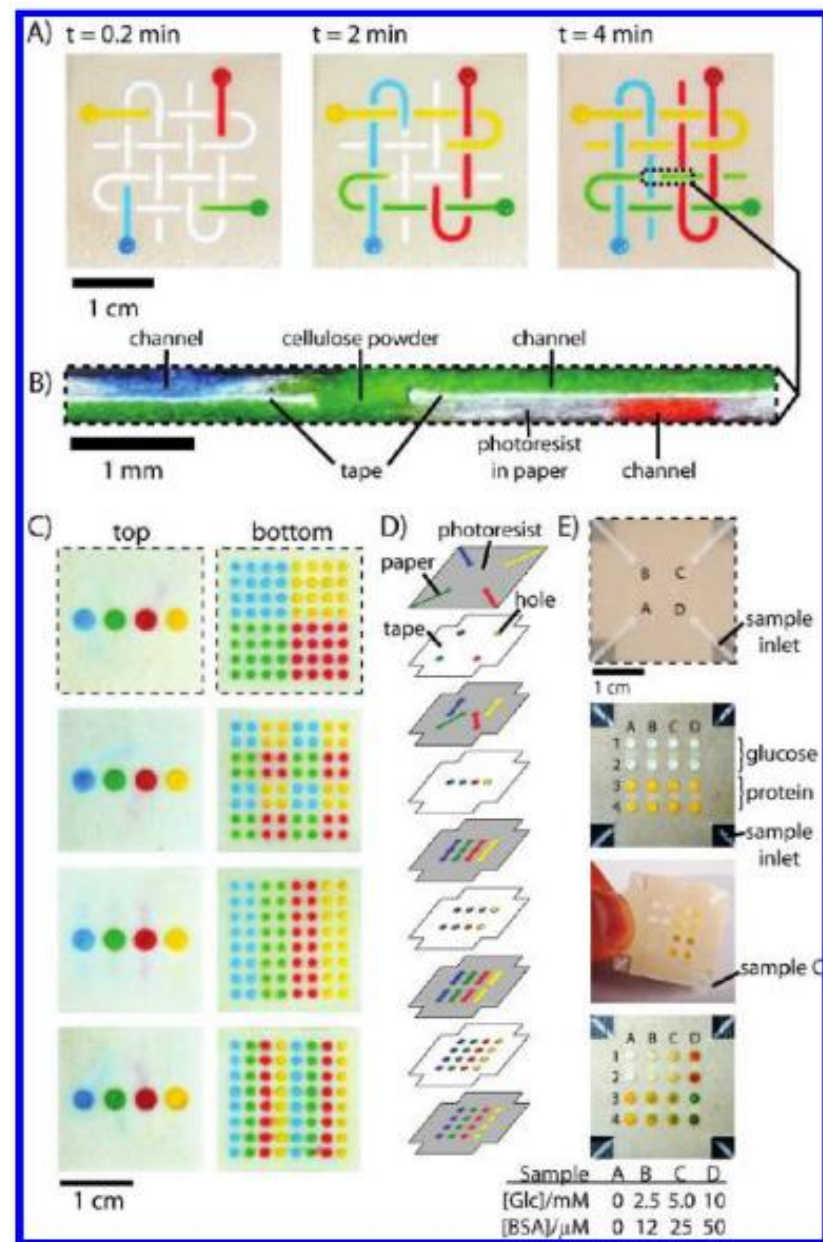


**Hydrophilic area for colorimetric detection**





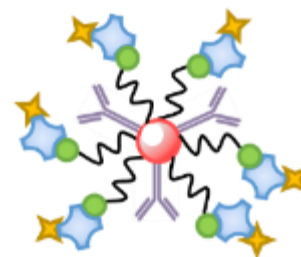
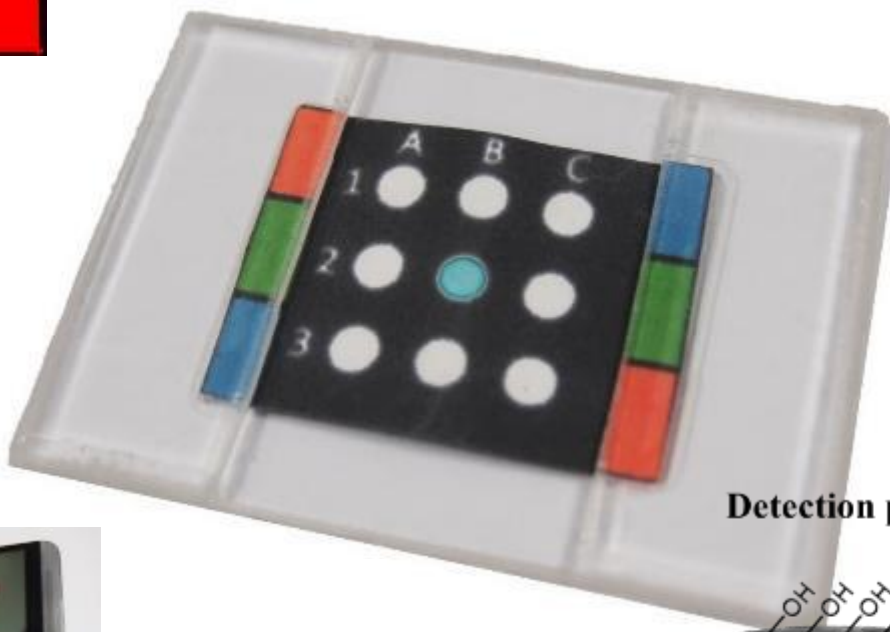
A) Image of a 96-zone plate after application of a range of volumes (1-55  $\mu\text{L}$ ) of solutions of aqueous dyes in alternating zones. B) Image showing the 96-zone plate with volumes of liquid up to 55  $\mu\text{L}$  that were completely contained by the hydrophobic barrier. C) Image of a 384-zone plate after application of 1-10  $\mu\text{L}$  of the same solutions as in (A). D) Image showing the 384-zone plate with volumes of fluid up to 10  $\mu\text{L}$  that were contained by the hydrophobic barrier. E) Image of a 96-zone plate with a serial dilution. F) Correlation of the absorbance values from a microplate reader and the gray scale values from an image acquired using a desktop scanner for the paper plate shown in (E).



*Analytical Chemistry*, 2009, 81, 5990–5998  
*Analytical Chemistry*, 2010, 82, 3-10

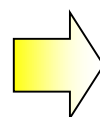
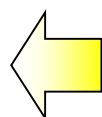


**Colorimetric or Electrical Sensing (capacitance or electrochemical)**



**Signal Amplification**

**System Integration**



Result readout

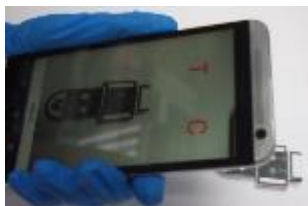
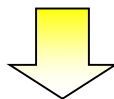
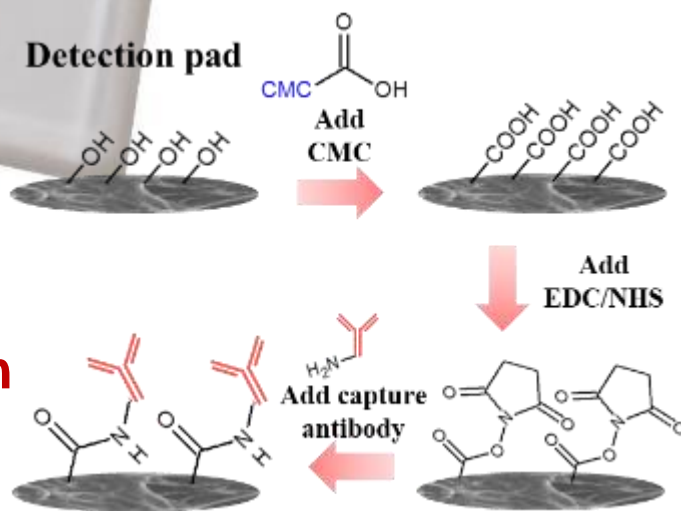


Image capture



**Surface Modification**

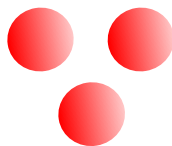


# Colorimetric Quantitative Detection on a Paper Device

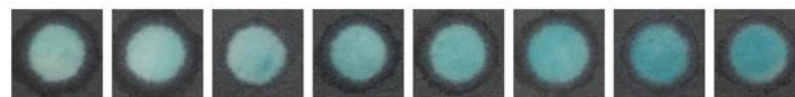


**\$ 20 K**

Surface plasmon resonance effect

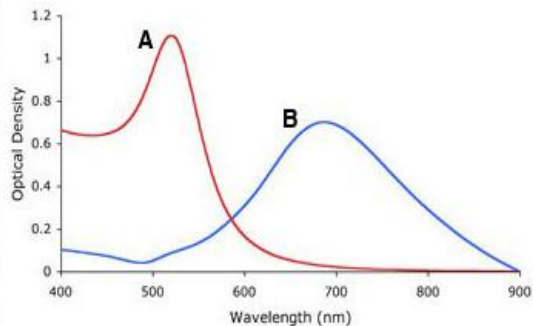
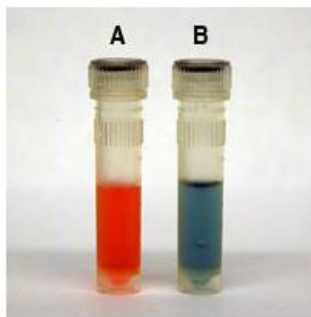


**\$ 0.2 K**

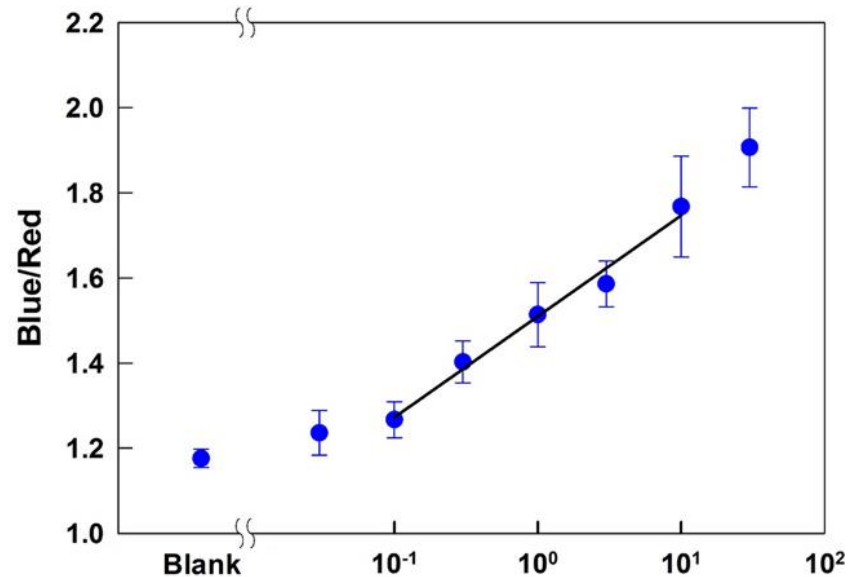


Blank 0.03 0.1 0.3 1 3 10 30

VS



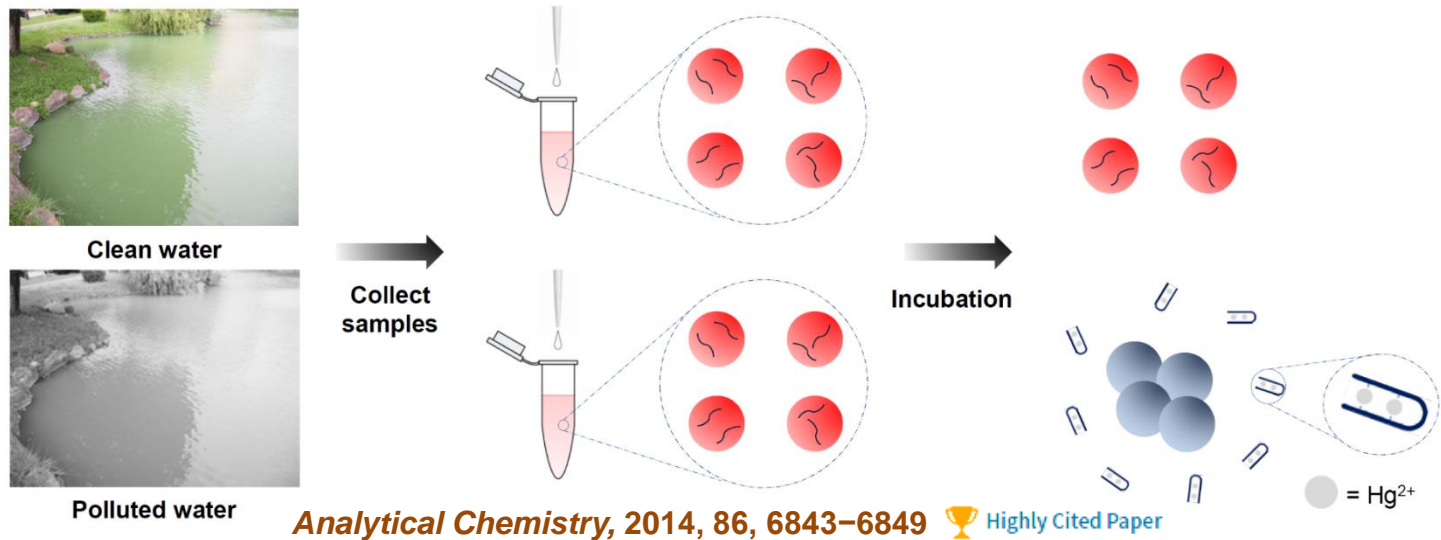
UV-Vis absorbance spectra



Colorimetric results readout of PADs

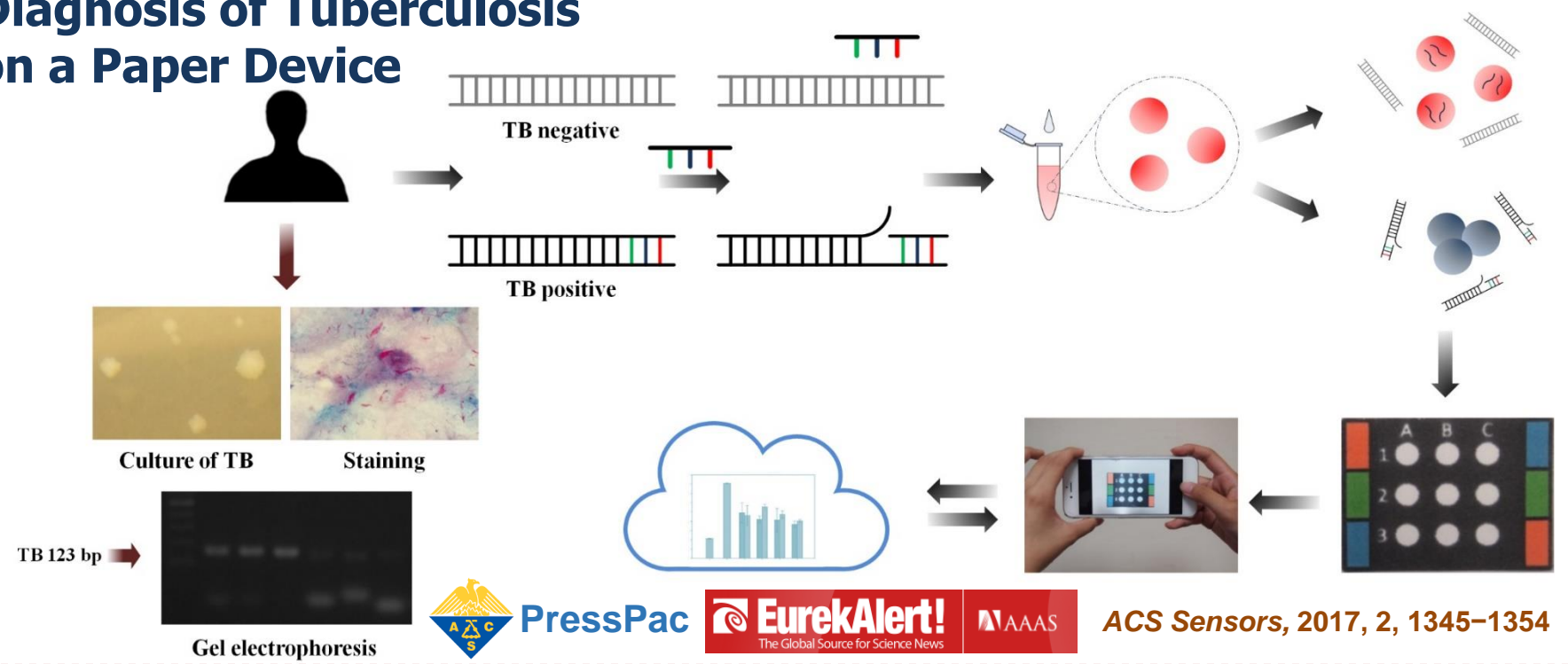


# On-Site $Hg^{2+}$ Sensing Using Colorimetric Au Nanoparticles on a Paper Device



*Analytical Chemistry*, 2014, 86, 6843–6849 Highly Cited Paper

# Diagnosis of Tuberculosis on a Paper Device





# Detection of Mercury(II) Ions Using Colorimetric Gold Nanoparticles on Paper-Based Analytical Devices

The colorimetric mechanism has been combined with label-free oligonucleotide sequences that can be attached to the AuNP surfaces via hydrophobic interaction and expose the negatively charged phosphate backbone to enhance resistance to the ion sheltering effect. However, when the surface-attached singlestranded DNA (ssDNA) sequences possess T-T mismatches, the addition of  $\text{Hg}^{2+}$  ions changes the structure of ssDNA into a hairpin structure based on T- $\text{Hg}^{2+}$ -T coordination chemistry. As a result, the zeta potential on the AuNP surfaces and the electrostatic repulsion between adjacent AuNPs were decreased; therefore, AuNPs aggregate in a salt solution. To obtain quantitative results, the blue/red ratio gained from the red-green-blue (RGB) values of each spot was calculated on the basis of the color change of the mixture, which was correlated with the different degrees of AuNPs aggregation and an increase in the concentration of  $\text{Hg}^{2+}$ .

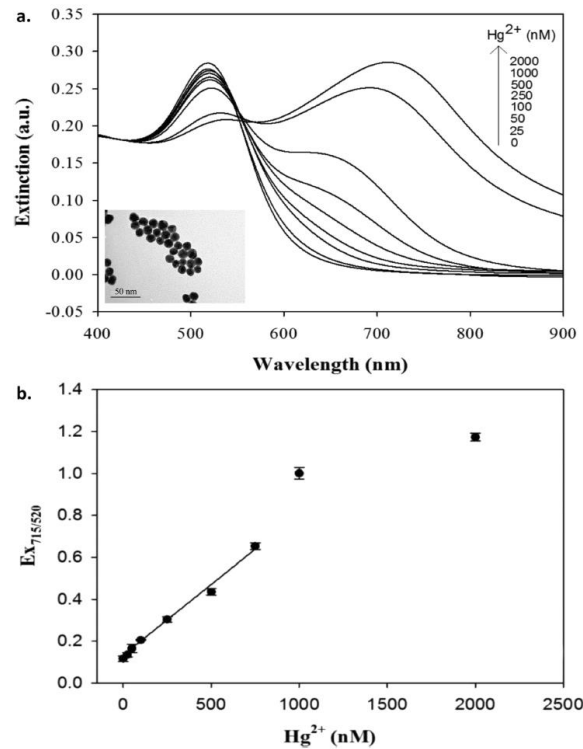


**Figure 1.** UV-vis absorbance spectra of colorimetric AuNPs and  $\text{Hg}^{2+}$ -ssDNA complex-based  $\text{Hg}^{2+}$  sensing. On the basis of the Ext 715/520 plot, the detection limit of 50 nM was obtained ( $n = 5$ ). A linear correlation is observed over the range of 25–750 nM ( $y = 0.0007x + 0.1272$  and  $R^2 = 0.98$ ).

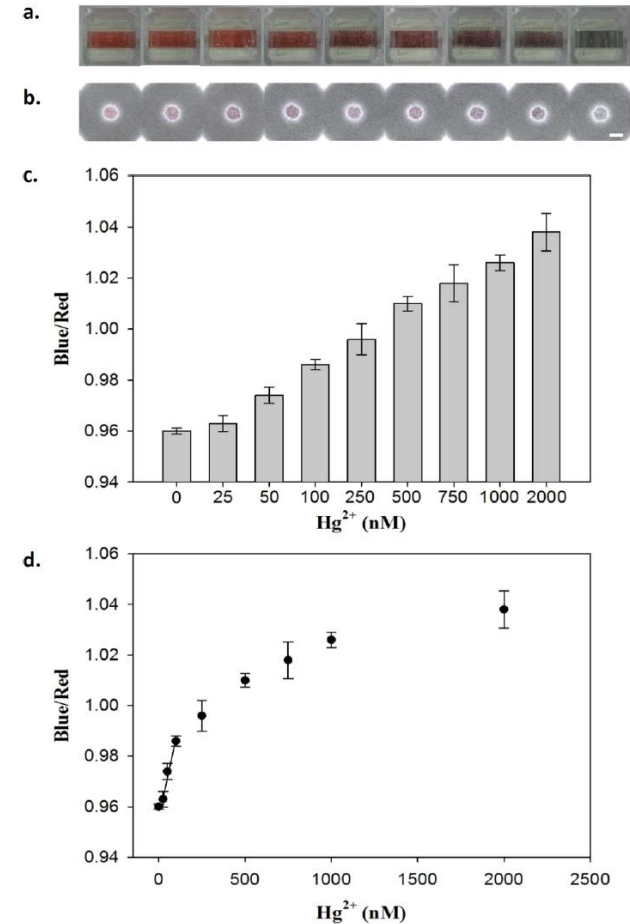


**Figure 2.** Colorimetric results for mercury ion detection (a) in cuvettes and (b) on cellulose paper. Panels (c) and (d) show the analytical blue/red color values of the spots. This paper-based colorimetric sensing platform has a detection limit of 50 nM, with a turnaround time of 40 min ( $n = 5$ ). The length of the inset scale bar is 3 mm.

# Detection of Mercury(II) Ions Using Colorimetric Gold Nanoparticles on Paper-Based Analytical Devices

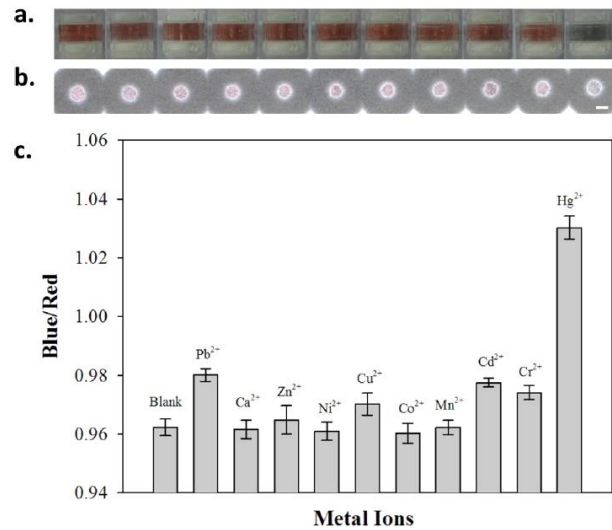


**Figure 4.** Specificity test results obtained for samples (a) in cuvettes and (b) on cellulose paper and (c) the analytical blue/red color values of the spots obtained using the proposed sensing platform. Although the concentrations of the other metal ions were 10-fold higher than the concentration of Hg<sup>2+</sup>, the blue/red values remain <1 ( $n = 5$ ). The length of the inset scale bar is 3 mm.

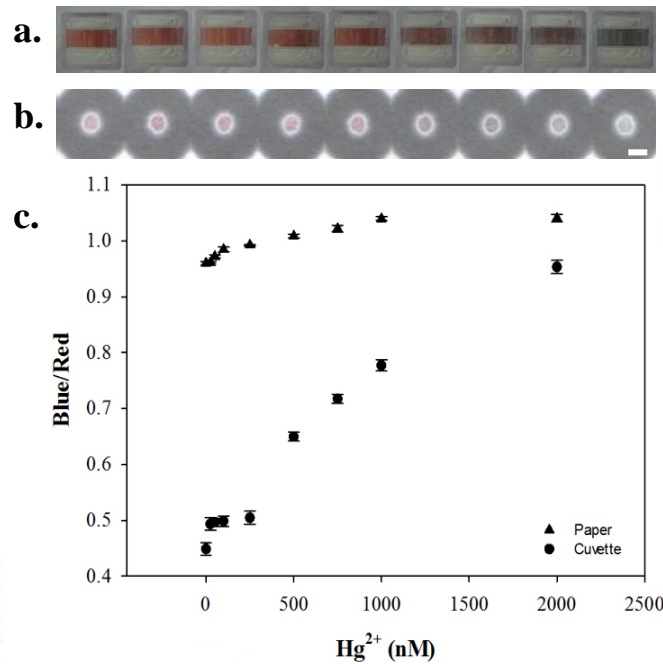


**Figure R1.** The colorimetric results for mercury ion detection (a) in cuvettes and (b) on cellulose paper and (c) the analytical blue/red color values of the cuvettes and spots. Both colorimetric value analyses have a detection limit of 50 nM ( $n=4$ ). The length of inset scale bar is 3 mm.

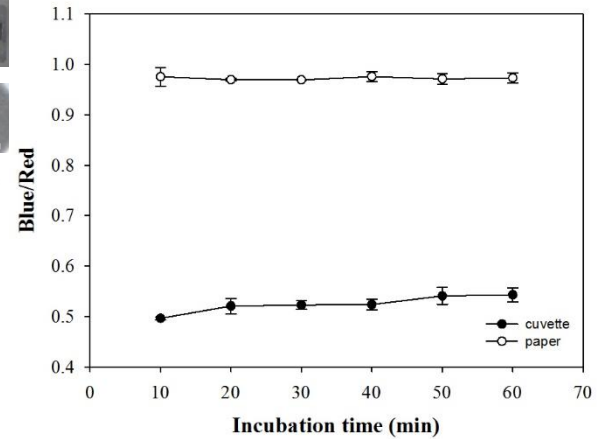


**Figure R2.** The colorimetric results for mercury ion detection in cuvettes and on cellulose paper. As color development time increase, the analytical blue/red color values of the spots reach stable after 20 min. In contrast, the values keep rising even the incubation time is at 60 min in cuvette. The concentration of Hg<sup>2+</sup> is 250 nM in ultrapure water ( $n=5$ ).

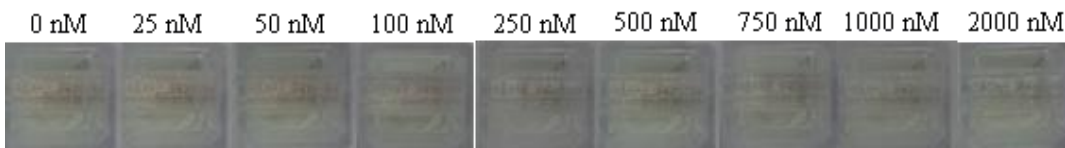


**Figure R3.** The colorimetric results for mercury ion detection in cuvettes using 100  $\mu$ L sample mixtures.

# Diagnosis of Tuberculosis Using Colorimetric Gold Nanoparticles on a Paper-Based Analytical Device

Effects of Heating Temperature, Denaturing Time, the Ratio of the Probe ssDNA to the Targeted dsDNA Sequences, and Different ssDNA Probe Sequences and Length

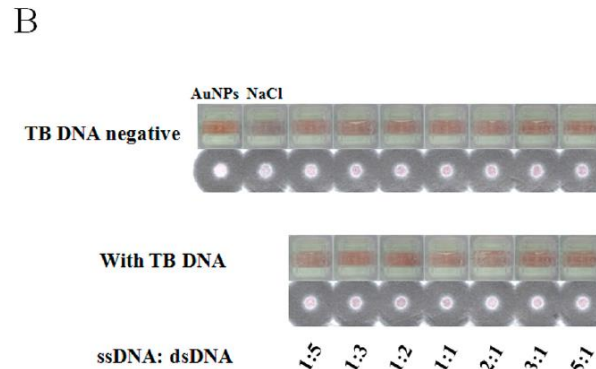
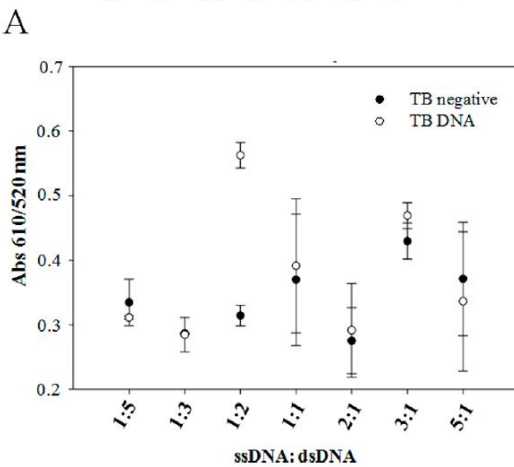
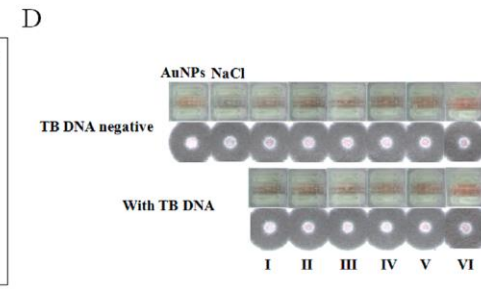
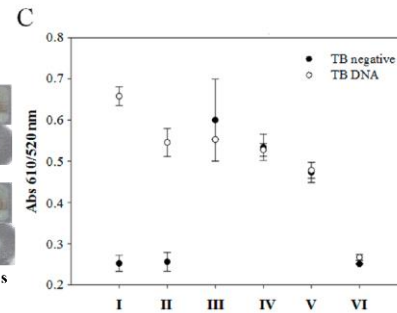
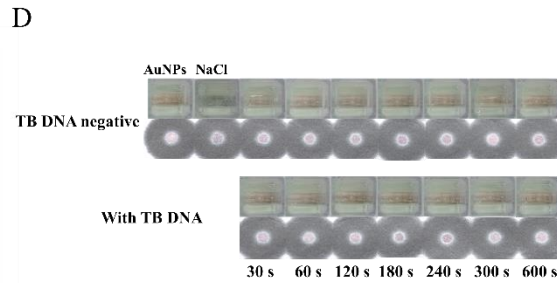
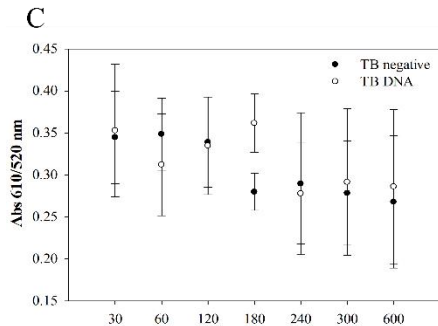
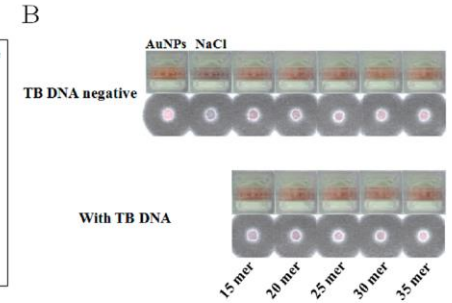
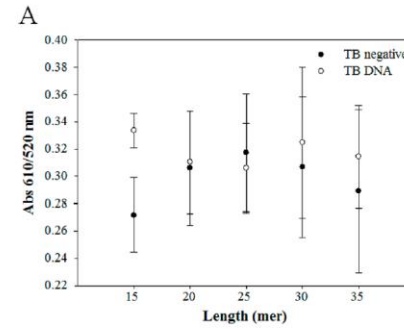
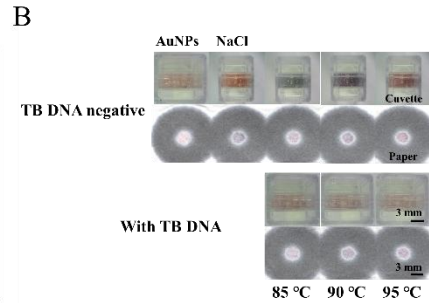
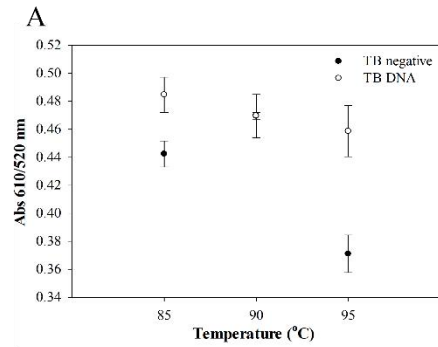
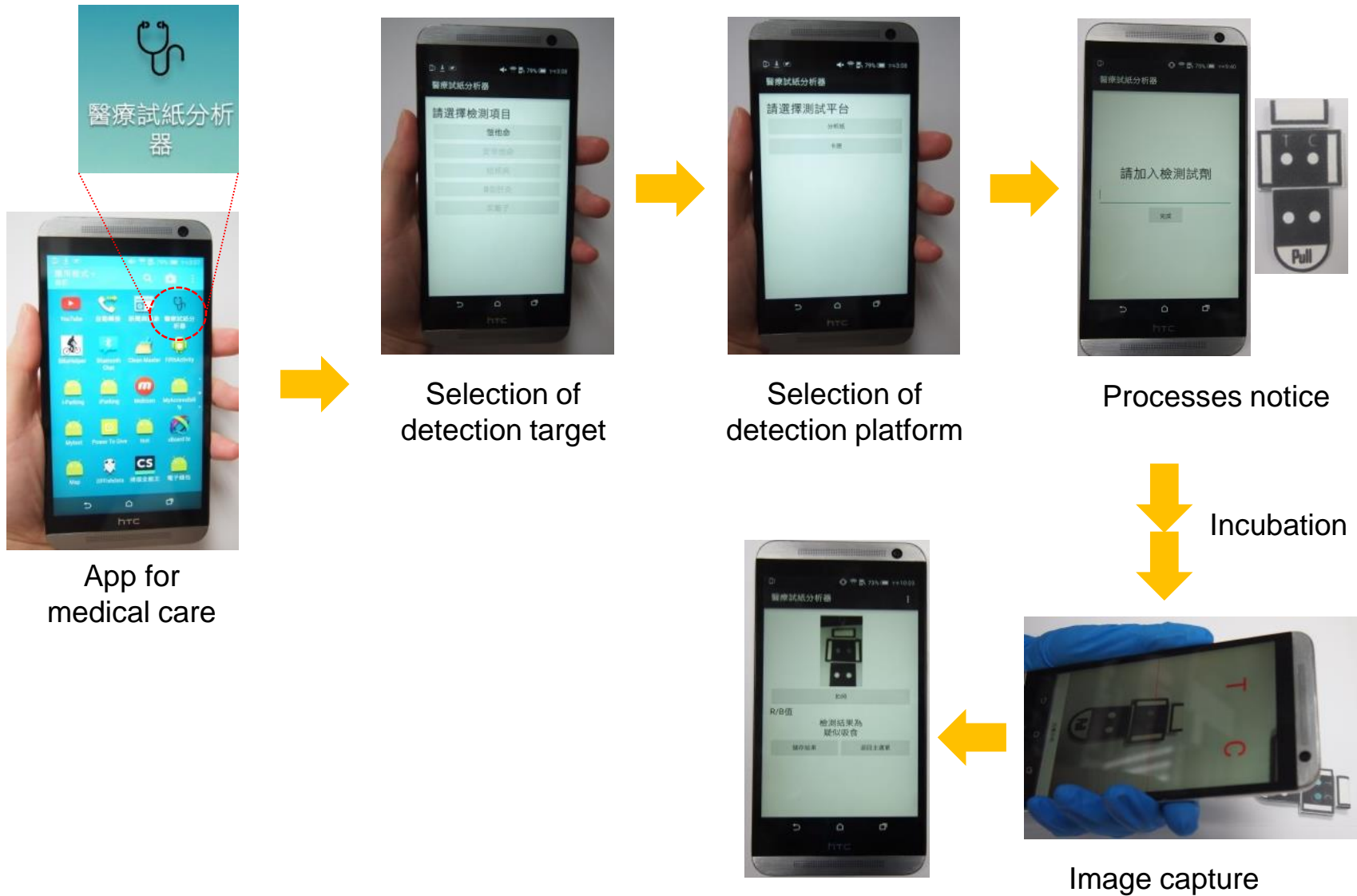


Table 1. Sequences of the Probe ssDNA for TB Analysis

primer name	sequence
RF15	5'-CCG AAG CGG CGC TGG-3'
RF20	5'-CCG AAG CGG CGC TGG ACG AG-3'
F15S10	5'-GCC GCT TCG GAC CAC-3'
F20S10	5'-GCC GCT TCG GAC CAC CAG CA-3'
RMU	5'-GGACCCGTCCCAAGCGGATG-3'
E20	5'-CCG ACG CCT ACG CTC GCA GG-3'
LMR	5'-CCTAACCGGCTGTGGGTAGC-3'
F25	5'-GTG GTC CGA AGC GGC GCT GGA CGA G-3'
F30	5'-TGC TGG TGG TCC GAA GCG GCG CTG GAC GAG-3'

# Smartphone Based Colorimetric Detection/Diagnosis



*Sensors & Actuators: B. Chemical, 2019, 282, 251-258.* Result readout



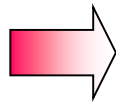
# On-Site Drug Detection

- ❖ In 2012, the Food and Drug Administration of Taiwan reported that 60% of reported drug abusers aged below 19 years old were addicted to ketamine.

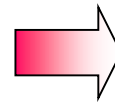


Blood test<sup>1</sup>

- **Invasive**
- **Infection risk**
- **Need trained and licensed personnel**



Sample preparation<sup>3</sup>



LC-MS/MS<sup>4</sup> or GC-MS/MS



Urine test<sup>2</sup>

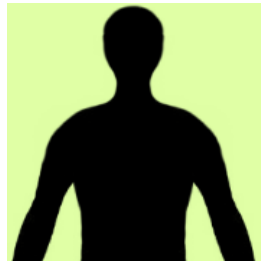
- **Adulteration**



- **Expensive**
- **Time consuming processes**
- **Bulky size of equipment**
- **Power sources requirement**

There is an urgent need for frontline officers to identify drug-impaired drivers at the roadside.

# Proposed Operation Processes



Suspect



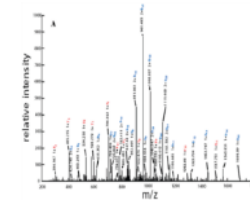
Oral fluid (OF) sampler



Put the OF samplers at the suspect's mouth



GC-MS/MS<sup>2</sup>



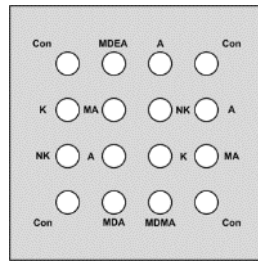
MS data



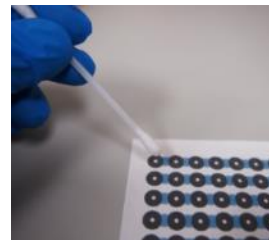
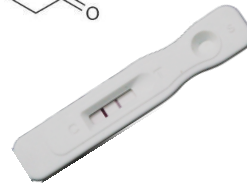
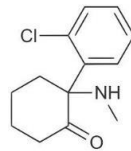
Police station



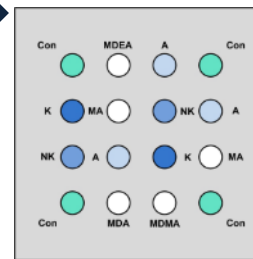
Pull over<sup>1</sup>



Microfluidic Paper-Based Analytical Devices (μPAD)



OF transferred to the μPAD and LFA



Colorimetric readout



Data capture and on-site analysis



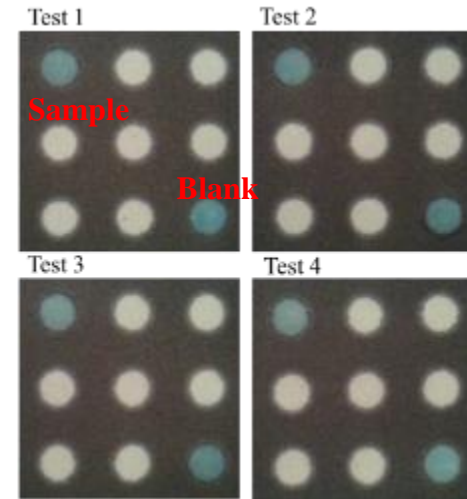
Cloud Computing

1. 東森新聞  
2. agilent.com  
3. appleapp.com  
4. plustek.com

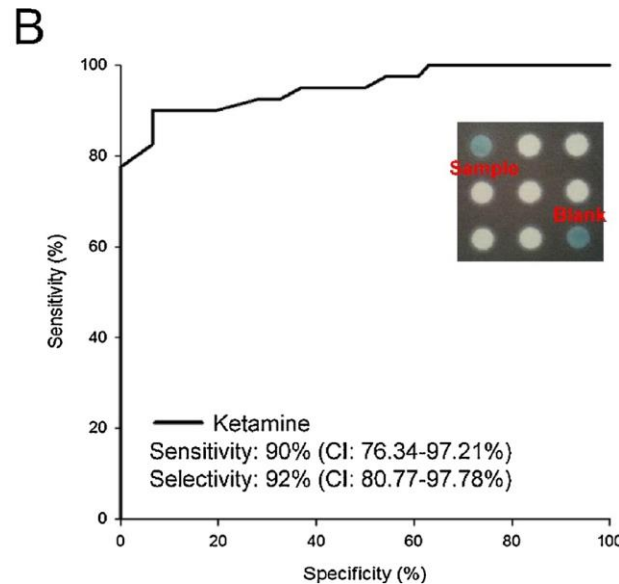
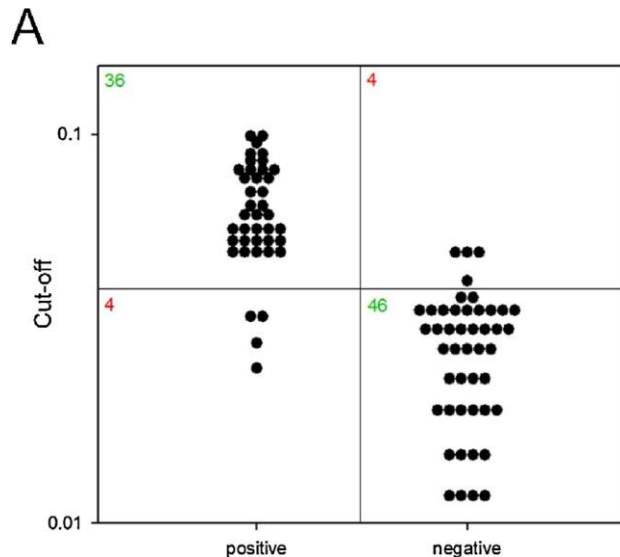
# Clinical Tests - $\mu$ PADs and LFAs

After optimization of the operation parameters, including reaction temperature, vibration washing time, reaction time, and antibody concentration, the resulting assay can be completed in as little as 6 min with a detection limit of 0.03 ng/mL.

Statistical results of (A) the cut-off point and (B) ROC curve from the cP-ELISA sensing system for clinical ketamine analysis. The cut-off value was 0.04, which resulted in a sensitivity and specificity for the platform of 90% (CI: 76.34–97.21%) and 92% (CI: 80.77–97.78%), respectively.

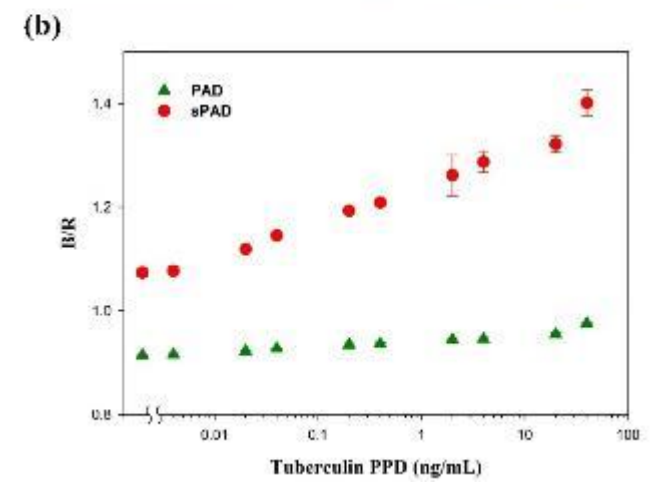
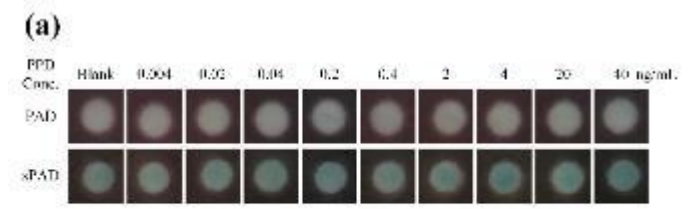
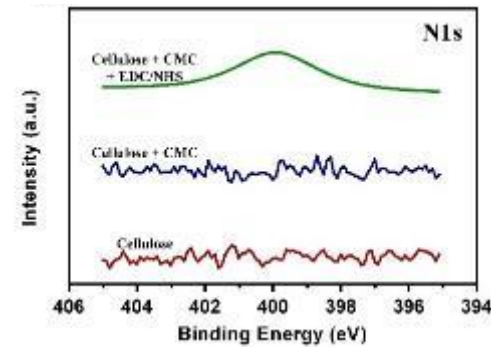
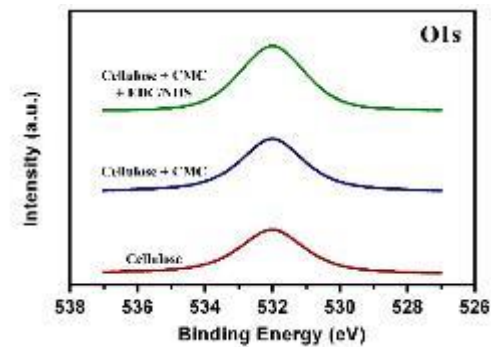
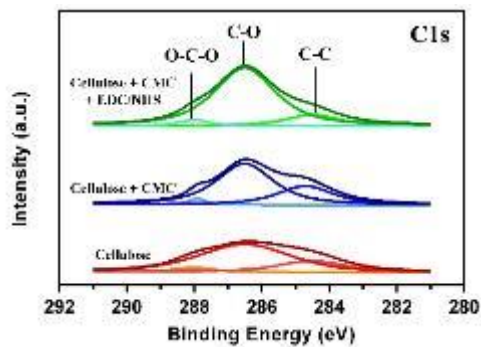
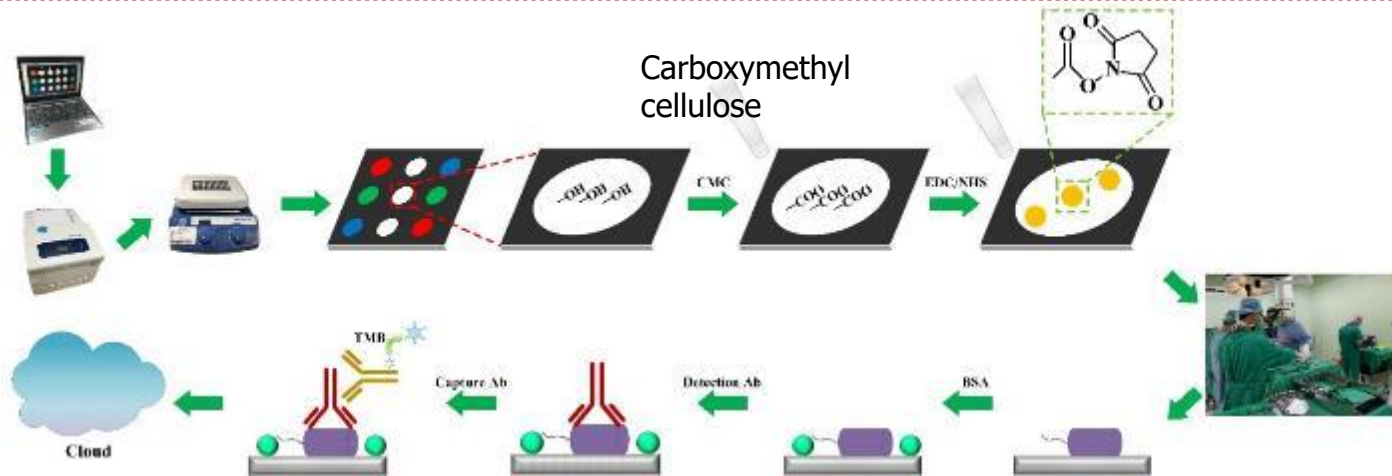


Clinical tests of  $\mu$ PADs



$R/B$  (Sample- Blank)  $\geq 0.04$   
→ Positive  
**Sensitivity = 85.7 %**  
**Specificity = 90 %**

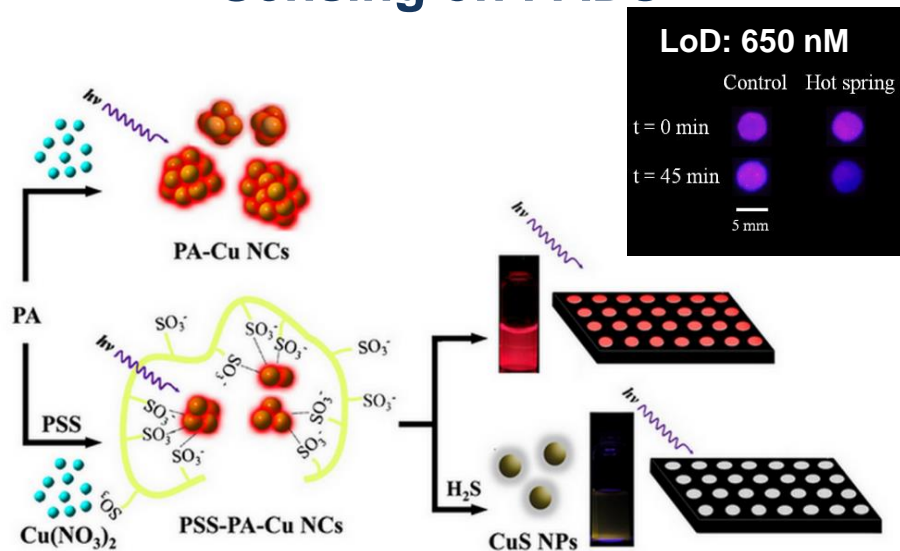
# Surface-Modified Cellulose Paper and Its Application in Disease Diagnosis



*Sensors and Actuators B: Chemical*, 2018, 506-513

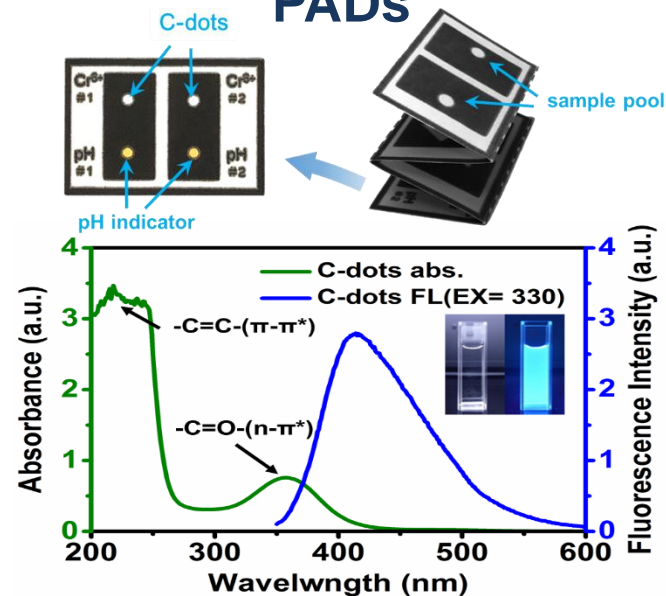


## Copper Nanocluster for H<sub>2</sub>S Sensing on PADs



*Scientific Reports*, 2016, 24882

## Carbon Dots for Cr<sup>6+</sup> Sensing on PADs

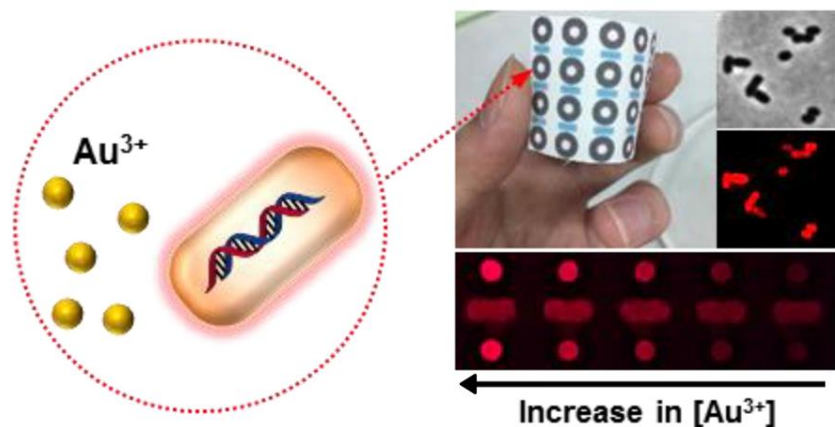


*Microchimica Acta*, 2019, 186, 227

## Microorganisms for Au ions Sensing on PADs

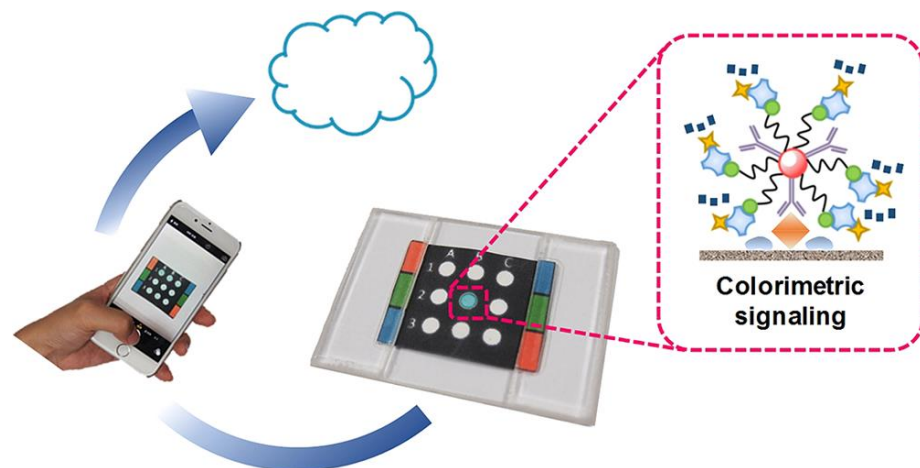
Microbial sensors

Paper device



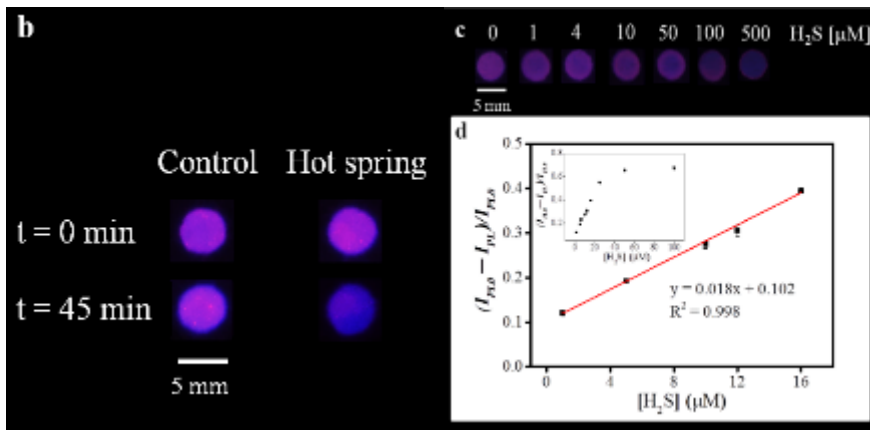
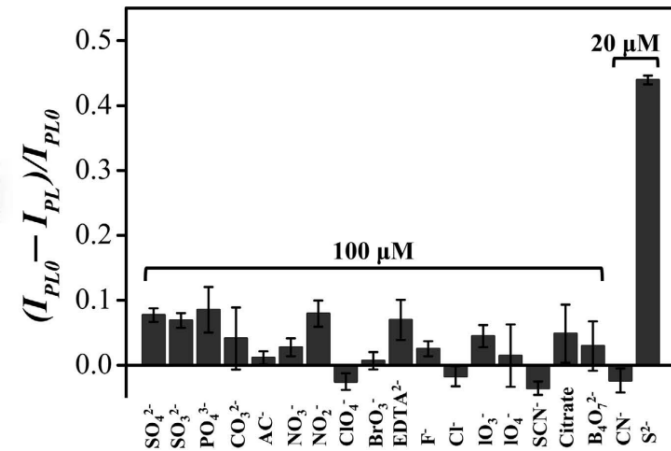
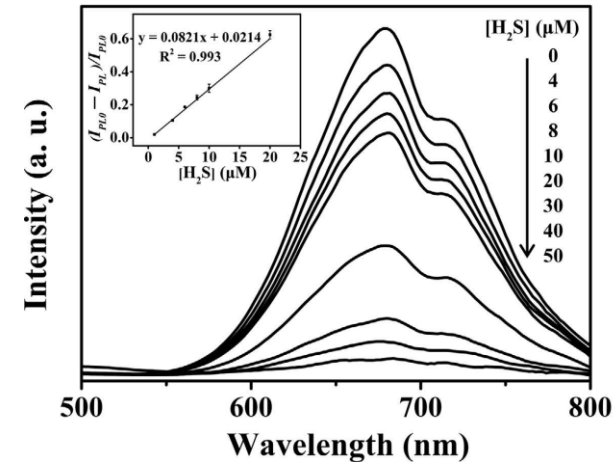
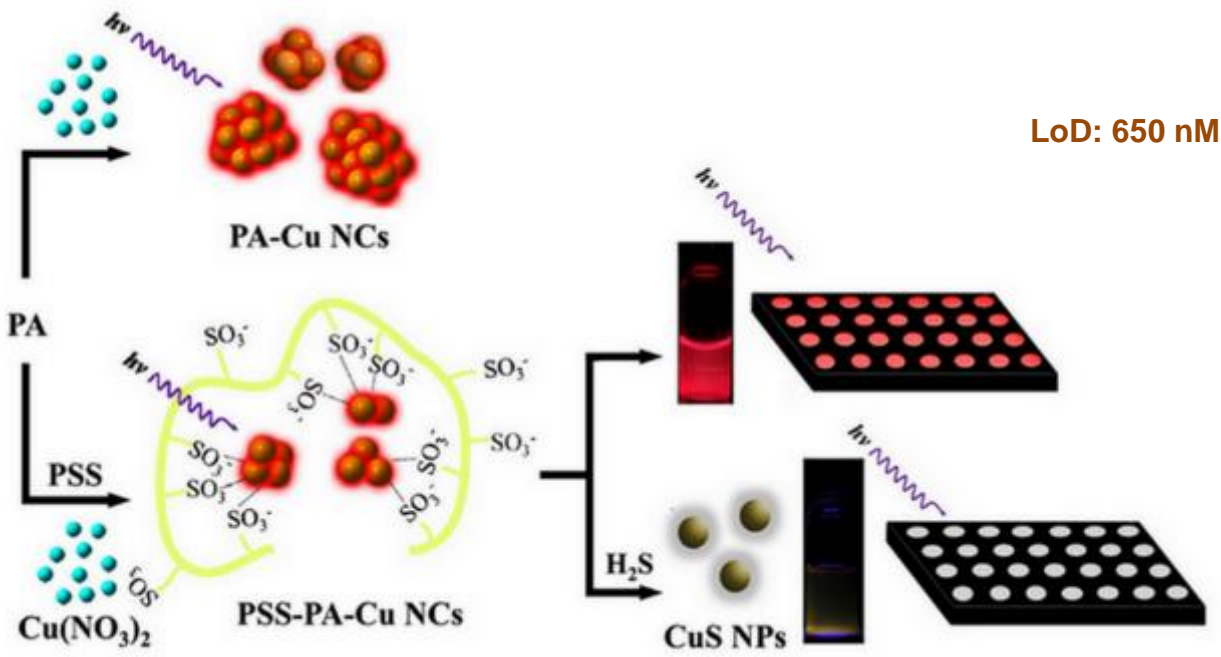
*ACS Sensors*, 2018, 3, 744–748

## Signal Amplified Au Nanoprobes



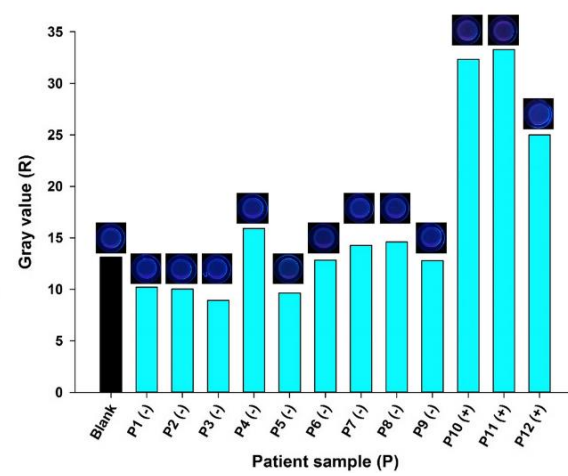
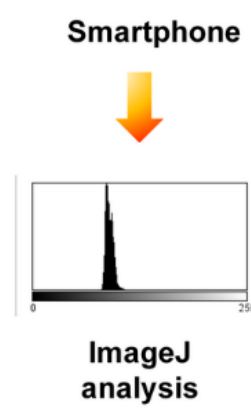
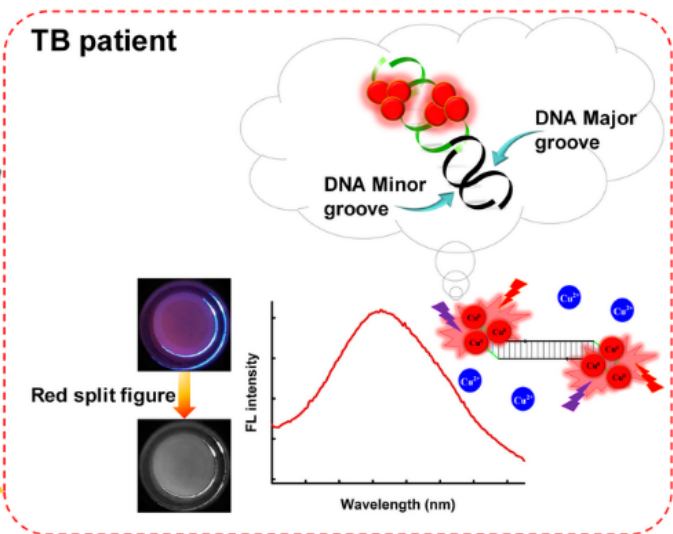
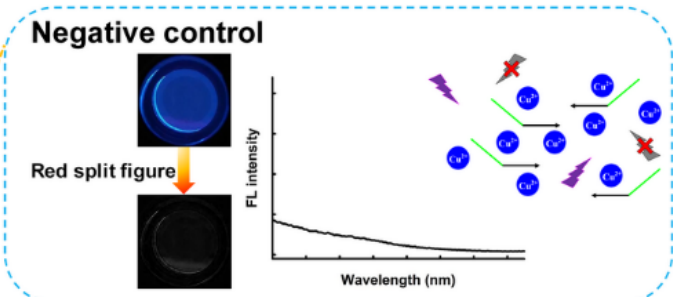
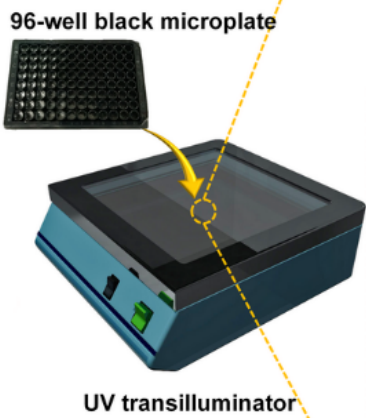
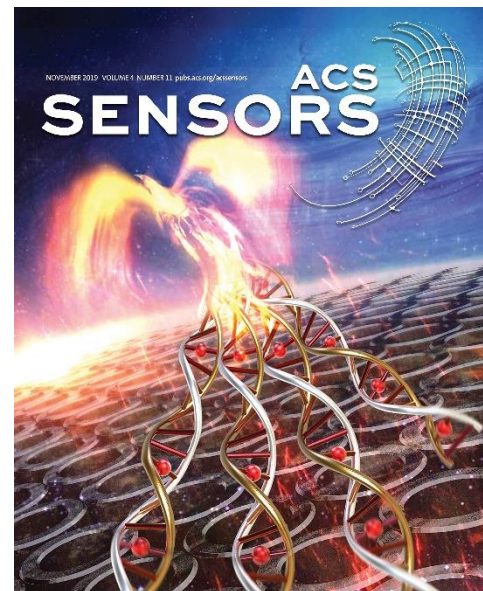
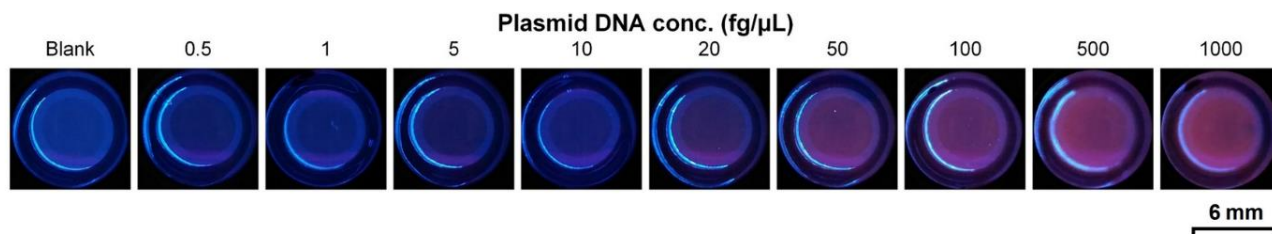
*ACS Sensors*, 2018, 3, 174–182

# Polystyrene Sulfonate Penicillamine-Copper Nanocluster Aggregates for H<sub>2</sub>S Sensing on PADs



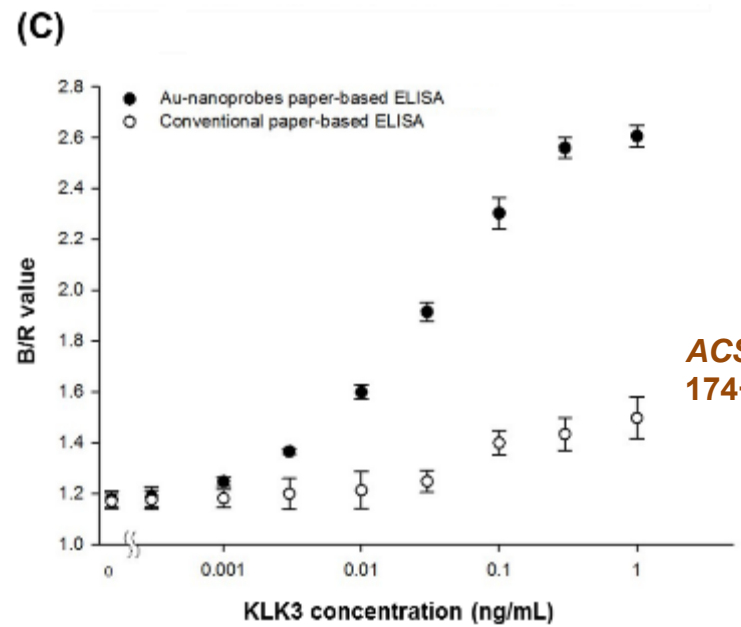
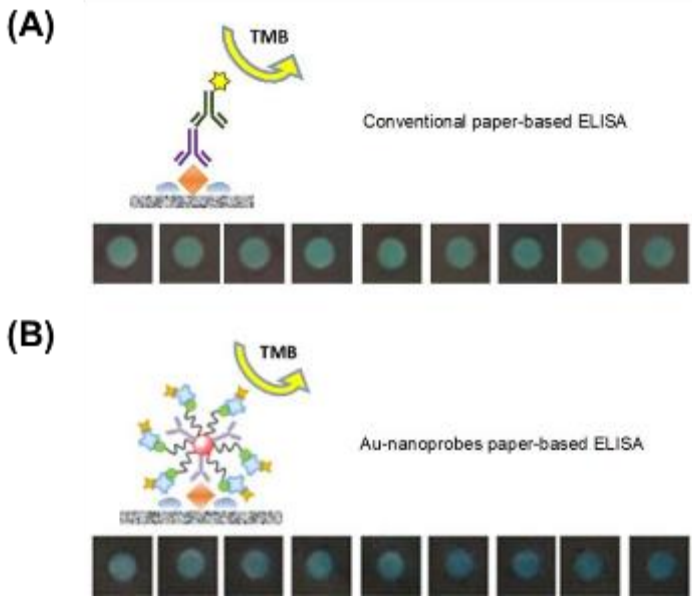
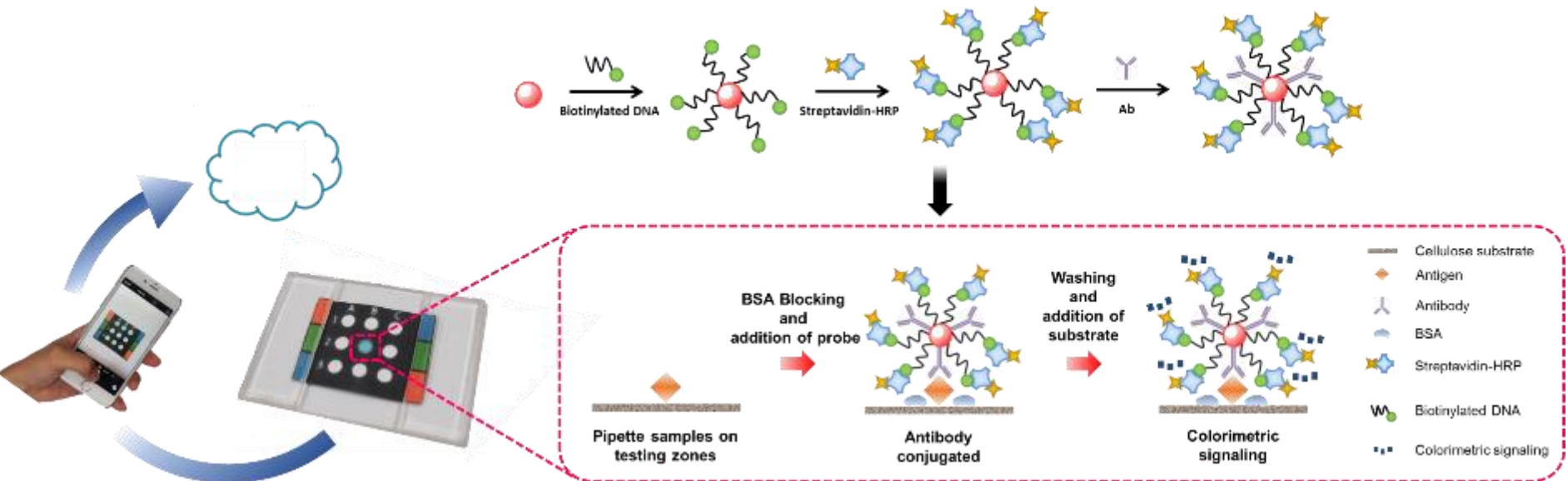
•The PSS-PA-Cu NCs were integrated into a portable μPAD for the on/off determination of H<sub>2</sub>S in water samples.

# Fluorescent Double-Stranded DNA-Templated Copper Nanoprobes for Rapid Diagnosis of Tuberculosis





# Signal Amplified Gold Nanoparticles for Disease Diagnosis on a Paper-Based Analytical Device

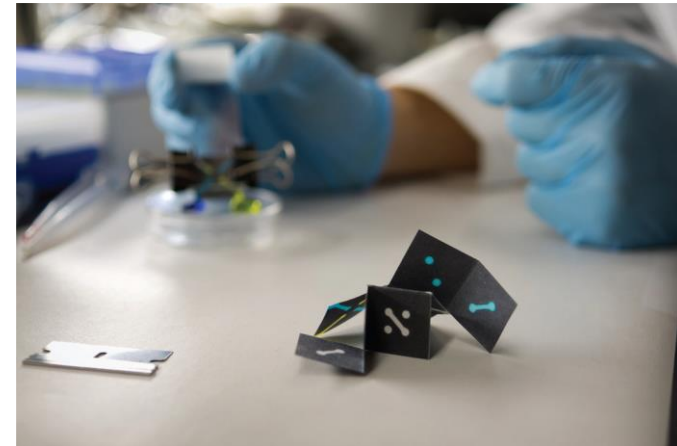
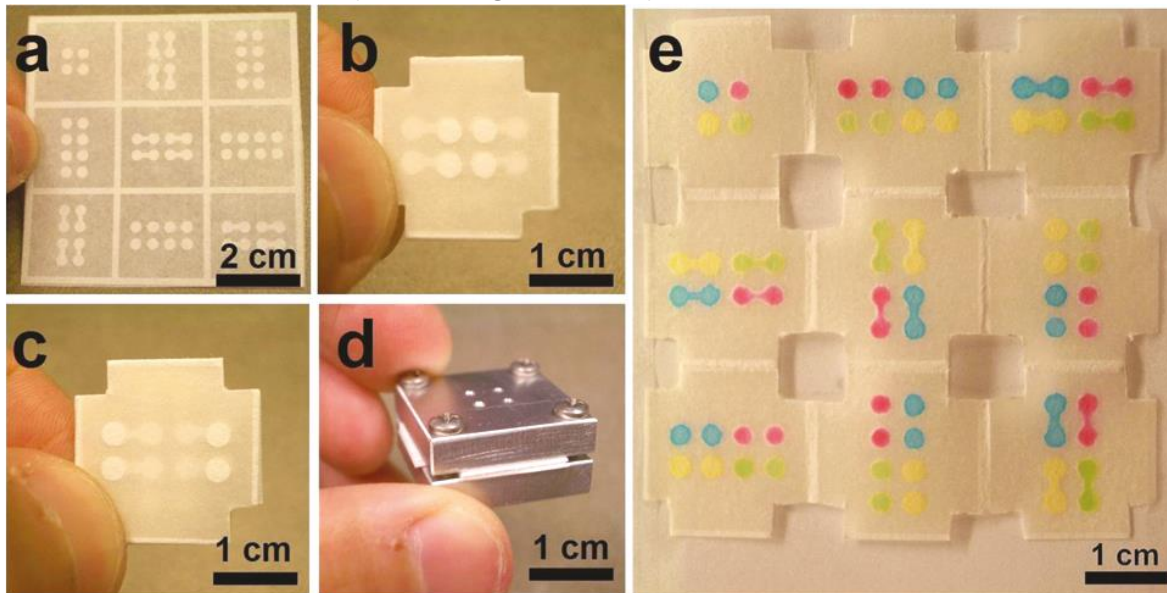


ACS Sensors, 2018, 3, 174–182



# Three-Dimensional Paper Microfluidic Devices Assembled Using the Principles of Origami

We report a method, based on the principles of origami (paper folding), for fabricating three-dimensional (3-D) paper microfluidic devices. The entire 3-D device is fabricated on a single sheet of flat paper in a single photolithographic step. It is assembled by simply folding the paper by hand. Following analysis, the device can be unfolded to reveal each layer. The applicability of the device to chemical analysis is demonstrated by colorimetric and fluorescence assays using multilayer microfluidic networks.

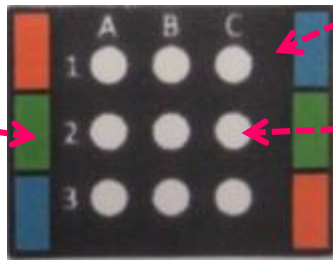


*J. Am. Chem. Soc.* 2011,  
133, 17564–17566

(a) Chromatography paper (100  $\mu\text{m}$  thick) having photolithographically patterned channels, reservoirs, and a folding frame. All channels were 900  $\mu\text{m}$  wide, and the reservoirs were 2.5 mm in diameter. (b) Top layer of the folded paper revealing four inlet reservoirs in the center of the device. The four flanking circular features are present within the 3-D structure of the device but are visible due to the transparency of the paper. Four corners of the folded paper were cut so it could be clamped in the aluminum housing shown in (d). (c) Bottom layer of the folded paper. (d) The aluminum housing used to support the 3-D paper microfluidic system. The four holes drilled in the top of the housing are used for injecting solutions. (e) An unfolded, nine-layer paper microfluidic device after injecting four 1.0 mM, aqueous, colored solutions through the four injection ports in the aluminum clamp.

# Three-dimensional origami paper-based device for portable immunoassay applications

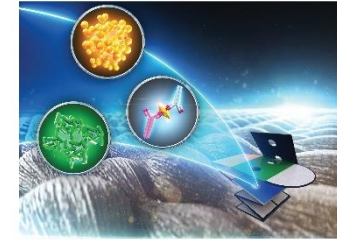
## Microfluidic Paper-Based Analytical Devices ( $\mu$ PADs)



**Hydrophobic wax for flow area definition**



**Hydrophilic area for colorimetric detection**






Learning unit from the International Journal of Food Microbiology and Food Safety, published by Elsevier, 2019.

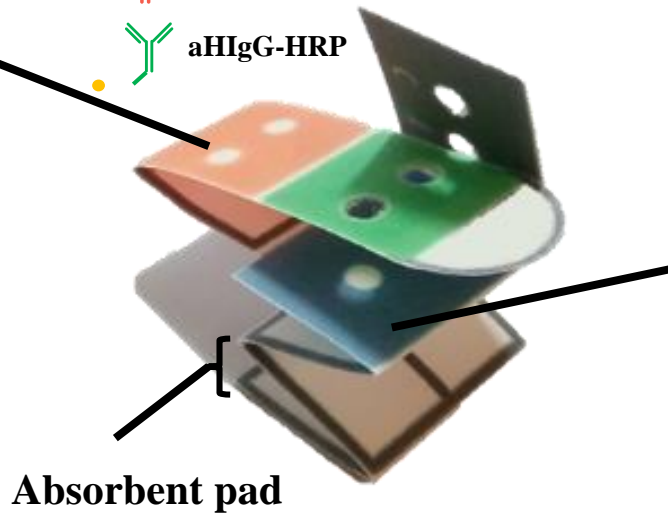
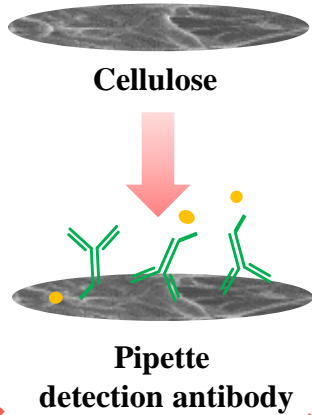


rsc.li/loc

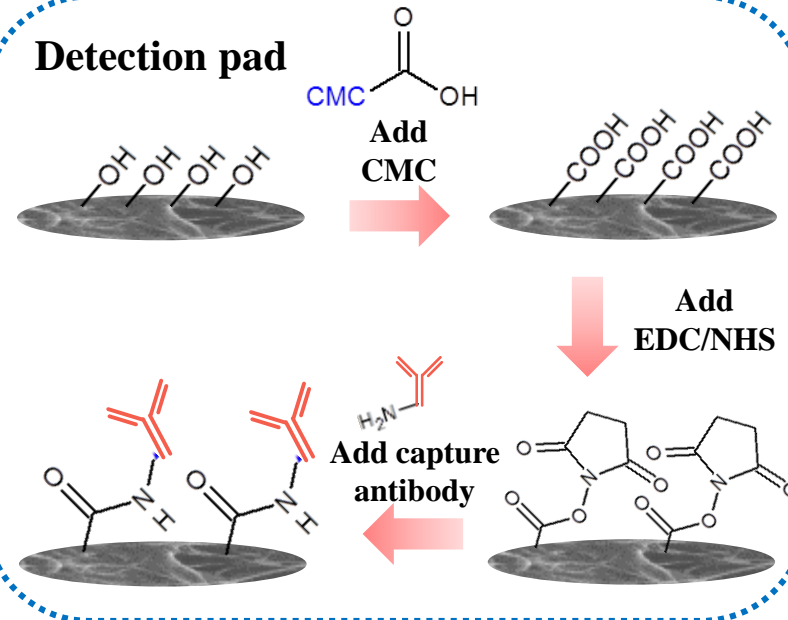
## Device design : 3D

-  cellulose
-  aHIgG Fab
-  aHIgG-HRP

### Conjugate pad

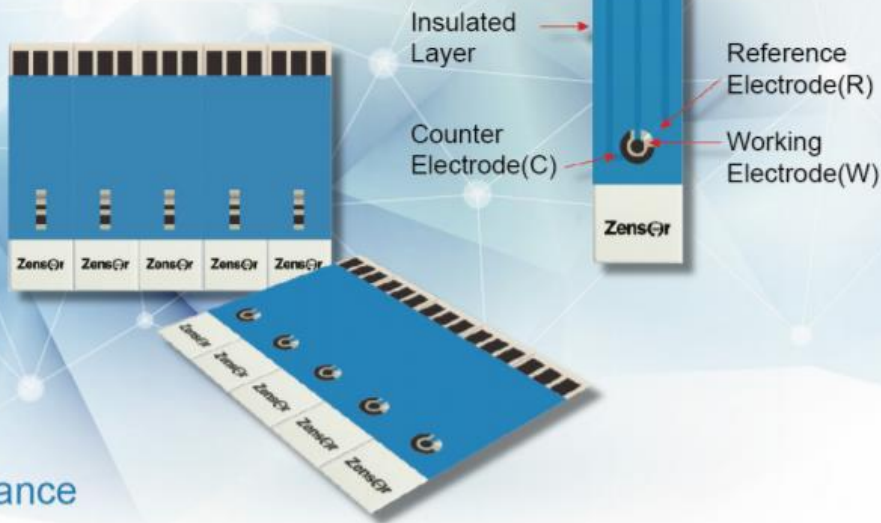


### Detection pad



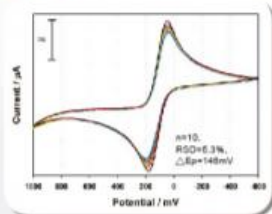
# 網版印刷碳電極

Screen-Printed Electrodes (Carbon)

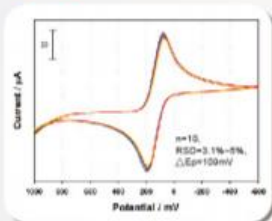


## Performance

### GCE



### TE100



Condition  
Solution : 3mM Ferricyanide, 0.1M KCl

## Specification

Type	Appearance	Model	Description (Diameter/Area)
Single Electrode		SE100	WE : 5mm / 0.196cm <sup>2</sup>
		SE101	WE : 3mm / 0.071cm <sup>2</sup>
		SE102	WE : 1.5mm / 0.018cm <sup>2</sup>
Three Electrode		TE100	WE : 3mm / 0.071cm <sup>2</sup> CE : Carbon ( 0.050cm <sup>2</sup> ) RE : Ag ( 0.010cm <sup>2</sup> )
		TE200	WE : 2x1mm / 0.020cm <sup>2</sup> CE : Carbon ( 0.040cm <sup>2</sup> ) RE : Ag ( 0.020cm <sup>2</sup> )

The **working electrode** works as an electron donor or acceptor to the analyte with the suitable potential in the electrolyte.

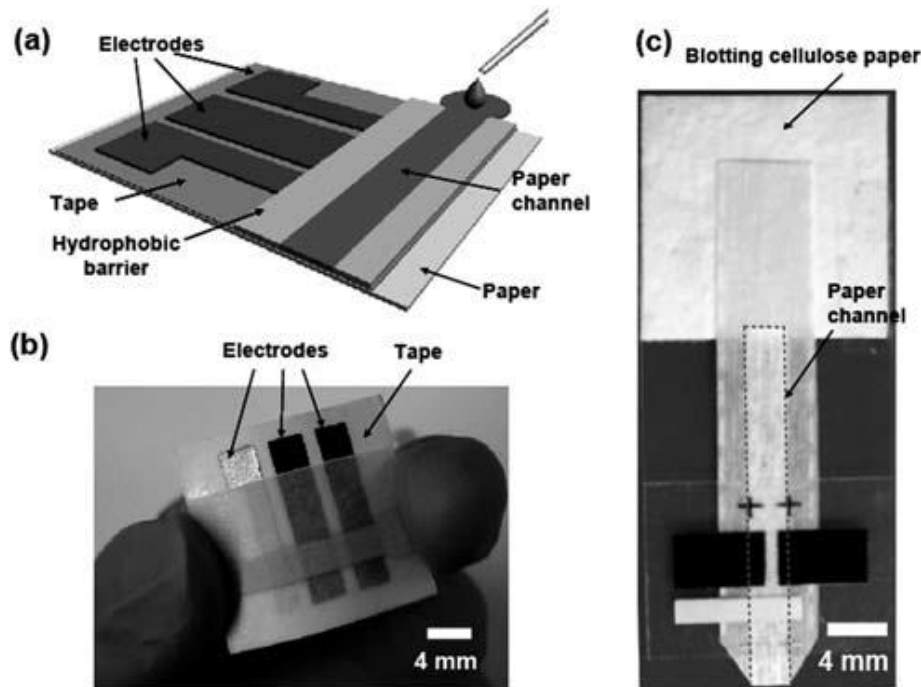
The **counter electrode** plays the opposite role to the working electrode, it should not participate with the electrochemical reaction except to balance the current observed at the working electrode.

A **reference electrode** is an electrode which has a stable and well-known electrode potential.



# Electrochemical sensing in paper-based microfluidic devices

This paper describes the fabrication and the performance of microfluidic paper-based electrochemical sensing devices (we call the **microfluidic paper-based electrochemical devices, mPEDs**). The mPEDs comprise paper-based **microfluidic channels patterned by photolithography or wax printing**, and **electrodes screen-printed from conducting inks (e.g., carbon or Ag/AgCl)**. We demonstrated that the mPEDs are capable of quantifying the concentrations of various analytes (e.g., heavy-metal ions and glucose) in aqueous solutions. This low-cost analytical device should be useful for applications in public health, environmental monitoring, and the developing world.

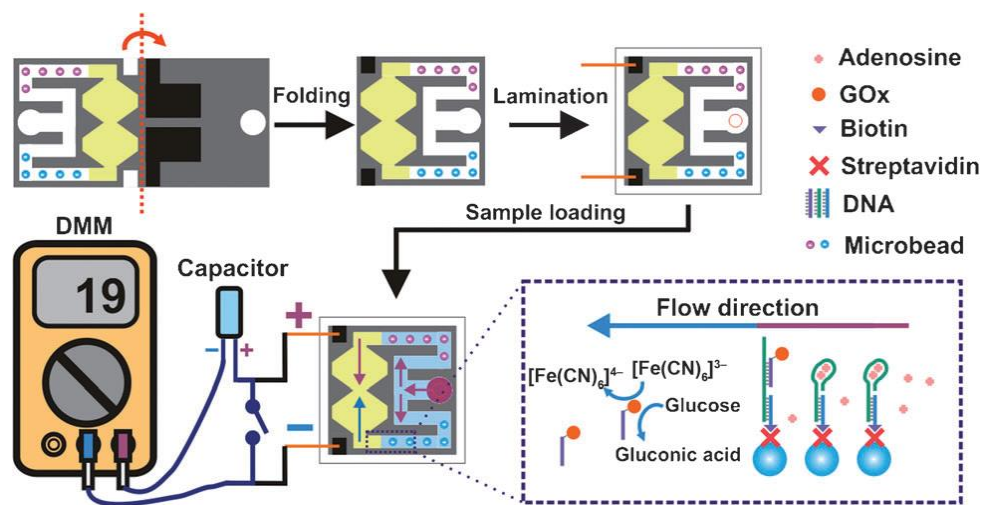


(a) Schematic of a paper-based electrochemical sensing device. The sensor comprises three electrodes printed on a piece of paper substrate (or plastic) and a paper channel. The paper channel was in conformal contact with the electrodes, and was held in place by double-sided adhesive tape surrounding the electrodes. A photograph of a paper-based electrochemical sensing device for the analysis of glucose (b), and a hydrodynamic paper-based electrochemical sensing device for the measurement of heavy-metal ions (c). The device consists of two printed carbon electrodes as the working and counter electrodes, and a printed Ag/AgCl electrode as the pseudo-reference electrode. The paper channel was fabricated by patterning SU-8 as a hydrophobic barrier for aqueous solution. The paper channel in (b) was colored with red ink to enhance imaging. The dashed line in (c) indicates the edge of the paper channel. The scale bar is 4 mm.

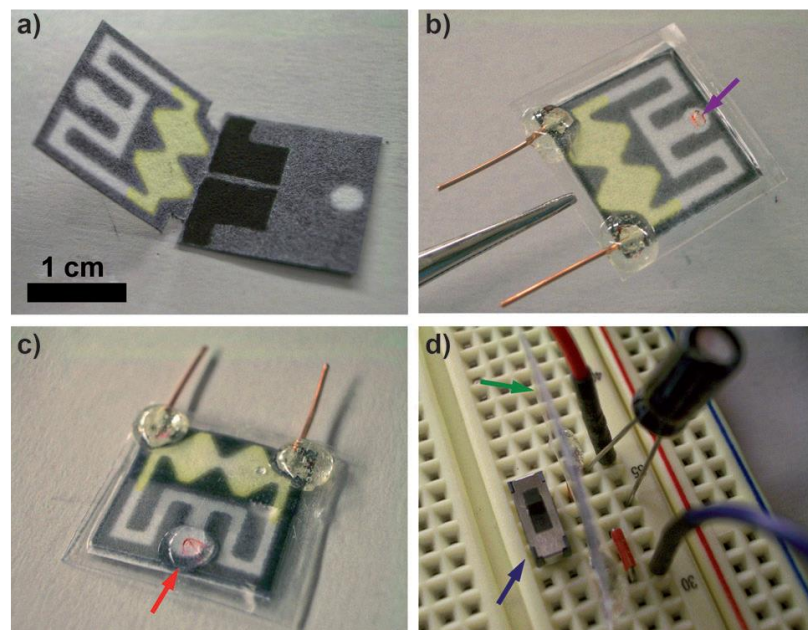


# Aptamer-Based Origami Paper Analytical Device for Electrochemical Detection of Adenosine

A self-powered origami paper analytical device (oPAD) uses an **aptamer** to recognize an analyte, a **glucose oxidase (GOx)** tag to modify the relative concentrations of an electroactive redox couple, and a **digital multimeter (DMM)** to transduce the result of the assay. The sensor is self-powered in that it self-generates an electrical signal so that the read-out process is similar to testing a battery



The operating principle of the sensor. DMM=digital multimeter.



a) A photograph of the unfolded oPAD fabricated by wax printing on chromatography paper. The two screen-printed carbon electrodes are visible on the bottom layer. The yellow color arises from the presence of  $[\text{Fe}(\text{CN})_6]^{3-}$  preloaded in the channel for the electrochemical assay. b) A photograph of the folded oPAD encapsulated in plastic using thermal edge lamination. The purple arrow indicates an opening for sample introduction, and the two copper wires are for electrical read-out. c) A photograph of the oPAD after introducing a 20 mL sample at the inlet (red arrow).

# A Paper-Based “Pop-up” Electrochemical Device for Analysis of Beta-Hydroxybutyrate

This paper describes the design and fabrication of a “pop-up” electrochemical paper-based analytical device (pop-up-EPAD) to measure beta-hydroxybutyrate (BHB)—a biomarker for diabetic ketoacidosis—using a commercial combination BHB/glucometer. Pop-up-EPADs are inspired by pop-up greeting cards and children’s books. They are made from a single sheet of paper folded into a three-dimensional (3D) device that changes shape, and fluidic and electrical connectivity, by simply folding and unfolding the structure. The reconfigurable 3D structure makes it possible to change the fluidic path and to control timing; it also provides mechanical support for the folded and unfolded structures that enables good registration and repeatability on folding. With simple modifications of the electrode and the design of the fluidic path, the pop-up-EPAD also detects BHB in buffer using a simple glucometer—a device that is more available than the combination BHB/glucometer.

Illustration of the process of testing BHB using “pop-up” paper test strips and a glucometer.

*Anal. Chem.* 2016, 88, 12, 6326–6333

